

A Two-Stage Learning-to-Defer Approach for Multi-Task Learning

Yannis Montreuil*

YANNIS.MONTREUIL@U.NUS.EDU

*School of Computing
National University of Singapore
Singapore, 118431, Singapore*

Yeo Shu Heng*

SHU.HENG@U.NUS.EDU

*School of Computing
National University of Singapore
Singapore, 118431, Singapore*

Axel Carlier

AXEL.CARLIER@TOULOUSE-INP.FR

*Institut de Recherche en Informatique de Toulouse
Institut national polytechnique de Toulouse
Toulouse, 31000, France*

Lai Xing Ng

NG_LAI_XING@I2R.A-STAR.EDU.SG

*Institute for Infocomm Research
Agency for Science, Technology and Research
Singapore, 138632, Singapore*

Wei Tsang Ooi

OOIWT@COMP.NUS.EDU.SG

*School of Computing
National University of Singapore
Singapore, 118431, Singapore*

Abstract

The Two-Stage Learning-to-Defer framework has been extensively studied for classification and, more recently, regression tasks. However, many contemporary applications involve both classification and regression in an interdependent manner. In this work, we introduce a novel Two-Stage Learning-to-Defer framework for multi-task learning that jointly addresses these tasks. Our approach leverages a two-stage surrogate loss family, which we prove to be both $(\mathcal{G}, \mathcal{R})$ -consistent and Bayes-consistent, providing strong theoretical guarantees of convergence to the Bayes-optimal rejector. We establish consistency bounds explicitly linked to the cross-entropy surrogate family and the L_1 -norm of the agents' costs, extending the theoretical minimizability gap analysis to the two-stage setting with multiple experts. We validate our framework on two challenging tasks: object detection, where classification and regression are tightly coupled, and existing methods fail, and electronic health record analysis, in which we highlight the suboptimality of current learning-to-defer approaches.

Keywords: Learning-to-Defer, Human-AI Collaboration, Machine Learning

1 Introduction

Learning-to-Defer (L2D) integrates predictive models with human experts—or, more broadly, decision-makers—to optimize systems requiring high reliability (Madras et al., 2018). This

*. These authors contributed equally to this work

approach benefits from the scalability of machine learning models and leverages expert knowledge to address complex queries (Hemmer et al., 2021). The Learning-to-Defer approach defers decisions to experts when the learning-based model has lower confidence than the most confident expert. This deference mechanism enhances safety, which is particularly crucial in high-stakes scenarios (Mozannar and Sontag, 2020; Mozannar et al., 2023). For example, in medical diagnostics, the system utilizes patient-acquired data to deliver an initial diagnosis (Johnson et al., 2023, 2016). If the model is sufficiently confident, its diagnosis is accepted; otherwise, the decision is deferred to a medical expert who provides the final diagnosis. Such tasks, which can directly impact human lives, underscore the need to develop reliable systems (Balagurunathan et al., 2021).

Learning-to-Defer has been extensively studied in classification problems (Madras et al., 2018; Verma et al., 2022; Mozannar and Sontag, 2020; Mozannar et al., 2023; Mao et al., 2023a) and, more recently, in regression scenarios (Mao et al., 2024e). However, many modern complex tasks involve both regression and classification components, requiring deferral to be applied to both components simultaneously, as they cannot be treated independently. For instance, in object detection, a model predicts both the class of an object and its location using a regressor, with these outputs being inherently interdependent (Girshick, 2015; Redmon et al., 2016; Buch et al., 2017). In practice, deferring only localization or classification is not meaningful, as decision-makers will treat these two tasks simultaneously. A failure in either component—such as misclassifying the object or inaccurately estimating its position—can undermine the entire problem, emphasizing the importance of coordinated deferral strategies that address both components jointly.

This potential for failure underscores the need for a Learning-to-Defer approach tailored to multi-task problems involving both classification and regression. We propose a novel framework for multi-task environments, incorporating expertise from multiple experts and the predictor-regressor model. We focus our work on the *two-stage scenario*, where the model is already trained offline. This setting is relevant when retraining from scratch the predictor-regressor model is either too costly or not feasible due to diverse constraints such as non-open models (Mao et al., 2023a, 2024e). We approximate the *true deferral loss* using a *surrogate deferral loss* family, based on cross-entropy, and tailored for the two-stage setting, ensuring that the loss effectively approximates the original discontinuous loss function. Our theoretical analysis establishes that our surrogate loss is both $(\mathcal{G}, \mathcal{R})$ -consistent and Bayes-consistent. Furthermore, we study and generalize results on the minimizability gap for deferral loss based on cross-entropy, providing deeper insights into its optimization properties.

Our contributions are as follows:

(i) **Novelty:** We introduce two-stage Learning-to-Defer for multi-task learning with multiple experts. Unlike previous L2D methods that focus solely on classification or regression, our approach addresses both tasks in a unified framework.

(ii) **Theoretical Foundation:** We prove that our surrogate family is both Bayes-consistent and $(\mathcal{G}, \mathcal{R})$ -consistent for any cross-entropy-based surrogate. We derive tight consistency bounds that depend on the choice of the surrogate and the L_1 -norm of the cost, extending minimizability gap analysis to the two-stage, multi-expert setting. Additionally, we establish learning bounds for the *true deferral loss*, showing that generalization improves as agents become more accurate.

(iii) **Empirical Validation:** We evaluate our approach on two challenging tasks. In object detection, our method effectively captures the intrinsic interdependence between classification and regression, overcoming the limitations of existing L2D approaches. In EHR analysis, we show that current L2D methods struggle when agents have varying expertise across classification and regression—whereas our method achieves superior performance.

2 Related Works

Learning-to-Defer builds on the foundational ideas of Learning with Abstention (Chow, 1970; Bartlett and Wegkamp, 2008; Cortes et al., 2016; Geifman and El-Yaniv, 2017; Ramaswamy et al., 2018; Cao et al., 2022; Mao et al., 2024a), where the primary goal is to reject inputs when the model lacks sufficient confidence. L2D extends this framework by incorporating a comparison between the model’s confidence and the confidence of experts.

One-stage L2D. Learning-to-Defer was first introduced by Madras et al. (2018), who proposed a pass function for binary classification, inspired by the *predictor-rejector* framework of Cortes et al. (2016). Extending this concept to the multi-class setting, Mozannar and Sontag (2020) proposed a *score-based* approach and demonstrated that employing a log-softmax multi-classification surrogate ensures a Bayes-consistent loss. Several subsequent works have further advanced or applied this methodology in classification tasks (Verma et al., 2022; Cao et al., 2024, 2022; Keswani et al., 2021; Kerrigan et al., 2021; Hemmer et al., 2022; Benz and Rodriguez, 2022; Tailor et al., 2024; Liu et al., 2024; Montreuil et al., 2024). A seminal contribution by Mozannar et al. (2023) identified limitations in prior approaches (Mozannar and Sontag, 2020; Verma et al., 2022), highlighting their suboptimality under realizable distributions. The authors argued that Bayes-consistency, while foundational, may not be the most reliable criterion in settings with a *restricted* hypothesis set. To address this, they proposed *hypothesis-consistency* as a more appropriate criterion in such scenarios. Building upon this paradigm, subsequent advances in hypothesis-consistency theory (Long and Servedio, 2013; Zhang and Agarwal, 2020; Awasthi et al., 2022; Mao et al., 2023b) have further refined the theoretical underpinnings of L2D. Notably, Mao et al. (2024c) established that the general score-based formulation of classification L2D is \mathcal{H} -consistent. Mao et al. (2024d) introduced a loss function achieving *realizable-consistency*, ensuring optimal performance under realizable distributions. Moreover, L2D has been successfully extended to regression tasks, with Mao et al. (2024e) demonstrating its applicability in multi-expert deferral settings.

Two-stage L2D. The increasing prominence of large pre-trained models has spurred interest in applying L2D to settings where agents (model and experts) are trained offline, reflecting the practical reality that most users lack the resources to train such models from scratch (Mao et al., 2023a; Montreuil et al., 2024). Charusaie et al. (2022) compared one-stage (online predictor) and two-stage (offline predictor) L2D approaches, identifying trade-offs between the two strategies. Mao et al. (2023a) proposed a predictor-rejector framework for two-stage L2D that guarantees both Bayes-consistency and hypothesis-consistency. Beyond classification, Mao et al. (2024e) extended the two-stage L2D framework to regression problems.

Despite significant progress, current two-stage L2D research largely addresses classification and regression independently. However, many contemporary tasks involve both regression and classification components, necessitating their joint optimization. In this work, we extend two-stage L2D to joint classifier-regressor models, addressing this critical gap.

3 Preliminaries

Multi-task scenario. We consider a multi-task setting encompassing both classification and regression problems. Let \mathcal{X} denote the input space, $\mathcal{Y} = \{1, \dots, n\}$ represent the set of n distinct classes, and $\mathcal{T} \subseteq \mathbb{R}$ denote the space of real-valued targets for regression. For compactness, each data point is represented as a triplet $z = (x, y, t) \in \mathcal{Z}$, where $\mathcal{Z} = \mathcal{X} \times \mathcal{Y} \times \mathcal{T}$. We assume the data is sampled independently and identically distributed (i.i.d.) from a distribution \mathcal{D} over \mathcal{Z} (Girshick, 2015; Redmon et al., 2016; Carion et al., 2020).

We define a *backbone* $w \in \mathcal{W}$, or shared feature extractor, such that $w : \mathcal{X} \rightarrow \mathcal{Q}$. For example, w can be a deep network that takes an input $x \in \mathcal{X}$ and produces a latent feature vector $q = w(x) \in \mathcal{Q}$. Next, we define a *classifier* $h \in \mathcal{H}$, representing all possible classification heads operating on \mathcal{Q} . Formally, h is a score function defined as $h : \mathcal{Q} \times \mathcal{Y} \rightarrow \mathbb{R}$, where the predicted class is $h(x) = \arg \max_{y \in \mathcal{Y}} h(q, y)$. Likewise, we define a *regressor* $f \in \mathcal{F}$, representing all regression heads, where $f : \mathcal{Q} \rightarrow \mathcal{T}$. These components are combined into a single multi-head network $g \in \mathcal{G}$, where $\mathcal{G} = \{g : g(x) = (h \circ w(x), f \circ w(x)) \mid w \in \mathcal{W}, h \in \mathcal{H}, f \in \mathcal{F}\}$. Hence, g jointly produces classification and regression outputs, $h(q)$ and $f(q)$, from the same latent representation $q = w(x)$.

Consistency in classification. In classification, the primary objective is to find a classifier $h \in \mathcal{H}$ that minimizes the true error $\mathcal{E}_{\ell_{01}}(h)$, defined as $\mathcal{E}_{\ell_{01}}(h) = \mathbb{E}_{(x,y)}[\ell_{01}(h(x), y)]$. The Bayes-optimal error is given by $\mathcal{E}_{\ell_{01}}^B(\mathcal{H}) = \inf_{h \in \mathcal{H}} \mathcal{E}_{\ell_{01}}(h)$. However, directly minimizing $\mathcal{E}_{\ell_{01}}(h)$ is challenging due to the non-differentiability of the *true multiclass* 0-1 loss (Zhang, 2002; Steinwart, 2007; Awasthi et al., 2022). This motivates the introduction of the cross-entropy *multiclass surrogate* family, denoted by $\Phi_{01}^\nu : \mathcal{H} \times \mathcal{X} \times \mathcal{Y} \rightarrow \mathbb{R}^+$, which provides a convex upper bound to the *true multiclass loss* ℓ_{01} . This family is parameterized by $\nu \geq 0$ and encompasses standard surrogate functions widely adopted in the community such as the MAE (Ghosh et al., 2017) or the log-softmax (Mohri et al., 2012).

$$\Phi_{01}^\nu = \begin{cases} \frac{1}{1-\nu} \left(\left[\sum_{y' \in \mathcal{Y}} e^{h(x,y')-h(x,y)} \right]^{1-\nu} - 1 \right) & \nu \neq 1 \\ \log \left(\sum_{y' \in \mathcal{Y}} e^{h(x,y')-h(x,y)} \right) & \nu = 1. \end{cases} \quad (1)$$

The corresponding surrogate error is defined as $\mathcal{E}_{\Phi_{01}^\nu}(h) = \mathbb{E}_{(x,y)}[\Phi_{01}^\nu(h(x), y)]$, with its optimal value given by $\mathcal{E}_{\Phi_{01}^\nu}^*(\mathcal{H}) = \inf_{h \in \mathcal{H}} \mathcal{E}_{\Phi_{01}^\nu}(h)$. A crucial property of a surrogate loss is *Bayes-consistency*, which guarantees that minimizing the surrogate generalization error also minimizes the true generalization error (Zhang, 2002; Steinwart, 2007; Bartlett et al., 2006; Tewari and Bartlett, 2007). Formally, Φ_{01}^ν is Bayes-consistent with respect to ℓ_{01} if,

for any sequence $\{h_k\}_{k \in \mathbb{N}} \subset \mathcal{H}$, the following implication holds:

$$\begin{aligned} \mathcal{E}_{\Phi_{01}^\nu}(h_k) - \mathcal{E}_{\Phi_{01}^\nu}^*(\mathcal{H}) &\xrightarrow{k \rightarrow \infty} 0 \\ \implies \mathcal{E}_{\ell_{01}}(h_k) - \mathcal{E}_{\ell_{01}}^B(\mathcal{H}) &\xrightarrow{k \rightarrow \infty} 0. \end{aligned} \quad (2)$$

This property assumes that $\mathcal{H} = \mathcal{H}_{\text{all}}$, a condition that does not necessarily hold for restricted hypothesis classes such as \mathcal{H}_{lin} or $\mathcal{H}_{\text{ReLU}}$ (Long and Servedio, 2013; Awasthi et al., 2022). To address this limitation, Awasthi et al. (2022) proposed \mathcal{H} -consistency bounds. These bounds depend on a non-decreasing function $\Gamma : \mathbb{R}^+ \rightarrow \mathbb{R}^+$ and are expressed as:

$$\begin{aligned} \mathcal{E}_{\Phi_{01}^\nu}(h) - \mathcal{E}_{\Phi_{01}^\nu}^*(\mathcal{H}) + \mathcal{U}_{\Phi_{01}^\nu}(\mathcal{H}) &\geq \\ \Gamma\left(\mathcal{E}_{\ell_{01}}(h) - \mathcal{E}_{\ell_{01}}^B(\mathcal{H}) + \mathcal{U}_{\ell_{01}}(\mathcal{H})\right), \end{aligned} \quad (3)$$

where the minimizability gap $\mathcal{U}_{\ell_{01}}(\mathcal{H})$ measures the disparity between the best-in-class generalization error and the expected pointwise minimum error: $\mathcal{U}_{\ell_{01}}(\mathcal{H}) = \mathcal{E}_{\ell_{01}}^B(\mathcal{H}) - \mathbb{E}_x[\inf_{h \in \mathcal{H}} \mathbb{E}_{y|x}[\ell_{01}(h(x), y)]]$. Notably, the minimizability gap vanishes when $\mathcal{H} = \mathcal{H}_{\text{all}}$ (Steinwart, 2007; Awasthi et al., 2022). In the asymptotic limit, inequality (3) guarantees the recovery of Bayes-consistency, aligning with the condition in (2).

4 Two-stage Multi-Task L2D: Theoretical Analysis

4.1 Formulating the Deferral Loss

We extend the two-stage predictor-rejector framework, originally proposed by Mao et al. (2023a), to a multi-task context. We define an *offline-trained model* represented by the multi-task model $g \in \mathcal{G}$ defined in Section 3. We consider J *offline-trained experts*, denoted as M_j for $j \in \{1, \dots, J\}$, where each expert produces predictions $m_j(x) = (m_j^h(x), m_j^f(x))$ with $m_j^h(x) \in \mathcal{Y}$ and $m_j^f(x) \in \mathcal{T}$. The predictions $m_j(x)$ belong to the corresponding prediction space \mathcal{M}_j , i.e., $m_j(x) \in \mathcal{M}_j$. The combined predictions of all J experts are represented as $m(x) = (m_1(x), \dots, m_J(x))$, which lies in the joint prediction space \mathcal{M} . We use the notation $[J] = \{1, \dots, J\}$ exclusively to denote the set of experts and define the agent space $\mathcal{A} = \{0\} \cup [J]$ with $|\mathcal{A}| = J + 1$, the number of agents (model and experts) that we have in our system.

To allocate the decision, we define a rejector function $r \in \mathcal{R}$, where $r : \mathcal{X} \times \mathcal{A} \rightarrow \mathbb{R}$. The rejector determines which agent should be assigned the decision by following the rule $r(x) = \arg \max_{j \in \mathcal{A}} r(x, j)$. This formulation naturally leads to the deferral loss $\ell_{\text{def}} : \mathcal{R} \times \mathcal{G} \times \mathcal{Z} \times \mathcal{M} \rightarrow \mathbb{R}^+$:

Definition 1 (True deferral loss). *Let an input $x \in \mathcal{X}$, for any $r \in \mathcal{R}$, we have the true deferral loss:*

$$\ell_{\text{def}}(r, g, m, z) = \sum_{j=0}^J c_j(g(x), m_j(x), z) 1_{r(x)=j},$$

with a bounded cost c_j that quantifies the cost of allocating a decision to the agent $j \in \mathcal{A}$. When the rejector $r \in \mathcal{R}$ predicts $r(x) = 0$, the decision is allocated to the multi-task model g . This allocation incurs a general cost c_0 , which is defined in this context as

$c_0(g(x), z) = \rho(g(x), z)$, where $\rho : \mathcal{Y} \times \mathcal{T} \times \mathcal{Z} \rightarrow \mathbb{R}^+$ represents a general function capturing the discrepancy between the model’s prediction $g(x)$ and the ground truth z . Conversely, when the rejector predicts $r(x) = j$ for some $j > 0$, the decision is deferred to expert j , resulting in a deferral cost c_j defined as $c_j(m_j(x), z) = \rho(m_j(x), z) + \beta_j$, where $m_j(x)$ denotes the prediction by expert j , and $\beta_j \geq 0$ accounts for the inherent cost associated with querying expert j . For example, β_j could reflect the resources, effort, or time required to obtain the expertise from expert j .

Optimal deferral rule: In Definition 1, we introduced the *true deferral loss*, ℓ_{def} , which we aim to minimize by identifying the Bayes rejector $r \in \mathcal{R}$ that minimizes the true error. To formalize this, we analyze the pointwise Bayes rejector $r^B(x)$, which minimizes the conditional risk $\mathcal{C}_{\ell_{\text{def}}}$. The true risk is given by $\mathcal{E}_{\ell_{\text{def}}}(g, r) = \mathbb{E}_x[\mathcal{C}_{\ell_{\text{def}}}(g, r, x)]$. The following Lemma 2 can be established.

Lemma 2 (Pointwise Bayes Rejector). *Given an input $x \in \mathcal{X}$ and a distribution \mathcal{D} , the optimal rejection rule that minimizes the conditional risk $\mathcal{C}_{\ell_{\text{def}}}$ associated with the true deferral loss ℓ_{def} is defined as:*

$$r^B(x) = \begin{cases} 0 & \text{if } \inf_{g \in \mathcal{G}} \mathbb{E}_{y,t|x}[c_0] \leq \min_{j \in [J]} \mathbb{E}_{y,t|x}[c_j] \\ j & \text{otherwise,} \end{cases}$$

The proof is provided in Appendix B. Lemma 2 establishes that the rejector $r \in \mathcal{R}$ optimally determines whether to utilize the multi-task model $g \in \mathcal{G}$ or to defer to the most cost-effective expert. Specifically, the rejector defers to the expert j that minimizes the expected deferral cost, $\mathbb{E}_{y,t|x}[c_j(g(x), m_j(x), z)]$, whenever the expected cost of the optimal multi-task model, $\inf_{g \in \mathcal{G}} \mathbb{E}_{y,t|x}[c_0(g(x), z)]$, exceeds the minimum expected cost of the most confident expert.

Although the *true deferral loss*, ℓ_{def} , and its corresponding Bayes rejector were introduced in Lemma 2, the practical computation of this rejector is hindered by the non-differentiability of ℓ_{def} (Zhang, 2002).

4.2 Surrogate Loss for Two-Stage Multi-Task L2D

Introducing the Surrogate: To address challenges analogous to those posed by discontinuous loss functions (Berkson, 1944; Cortes and Vapnik, 1995), we formalize surrogate losses with desirable analytical properties. Specifically, we use the cross-entropy *multiclass surrogate loss* $\Phi_{01}^\nu : \mathcal{R} \times \mathcal{X} \times \mathcal{A} \rightarrow \mathbb{R}^+$ that is convex and upper-bounds the *true multiclass loss* ℓ_{01} . This surrogate family is defined in Equation 1.

Mao et al. (2024e) introduced a convex, upper-bound surrogate for the *true deferral loss*. Building on this, we incorporate new costs c_j to capture the interdependence between classification and regression tasks. The resulting surrogate family, $\Phi_{\text{def}}^\nu : \mathcal{R} \times \mathcal{G} \times \mathcal{M} \times \mathcal{Z} \rightarrow \mathbb{R}^+$, yields Lemma 3:

Lemma 3 (Surrogate deferral losses). *Let $x \in \mathcal{X}$ be a given input and Φ_{01}^ν a multiclass surrogate loss family. The surrogate deferral losses Φ_{def}^ν for $J + 1$ agents are defined as:*

$$\Phi_{\text{def}}^\nu(r, g, m, z) = \sum_{j=0}^J \tau_j(g(x), m(x), z) \Phi_{01}^\nu(r, x, j), \quad (4)$$

with the aggregated costs $\tau_j(g(x), m(x), z) = \sum_{i=0}^J c_i(g(x), m_i(x), z) \mathbb{1}_{i \neq j}$.

The *surrogate deferral loss* family, Φ_{def}^ν , aggregates the weighted surrogate losses for each possible decision: deferring to one of the J experts or utilizing the model directly. The weights $\tau_{j \in \mathcal{A}}$ represent the cumulative costs associated with each deferral path. Specifically, the weight τ_0 captures the total deferral cost across all experts, serving as a baseline for deferral decisions. Conversely, the weights $\tau_{j \in [J]}$ quantify the combined cost of utilizing the model while deferring to all experts except expert j .

The proposed surrogate family is broadly applicable and only requires Φ_{01}^ν to admit an \mathcal{R} -consistency bound. Furthermore, the formulated costs c_j accommodate any multi-task setting.

Consistency of the Surrogate Losses: In Lemma 3, we established that the surrogate losses serve as a convex upper bound for the *true deferral loss*. However, it remains to be shown whether this surrogate family provides a faithful approximation of the target true loss, ℓ_{def} . Specifically, the relationship between $r^*(x)$, the pointwise optimal rejector minimizing a surrogate loss from the family, and $r^B(x)$, the pointwise Bayes-optimal rejector for the true loss, is not immediately evident. To address this, we analyze the discrepancy between the *surrogates' excess risk*, $\mathcal{E}_{\Phi_{\text{def}}^\nu}(g, r) - \mathcal{E}_{\Phi_{\text{def}}^\nu}^*(\mathcal{G}, \mathcal{R})$, and the *excess risk under the true loss*, $\mathcal{E}_{\ell_{\text{def}}}(g, r) - \mathcal{E}_{\ell_{\text{def}}}^B(\mathcal{G}, \mathcal{R})$. This analysis is critical for understanding the surrogates' consistency, as explored in prior works (Steinwart, 2007; Zhang, 2002; Bartlett et al., 2006; Awasthi et al., 2022).

Using consistency bounds from (Awasthi et al., 2022; Mao et al., 2024b), we present Theorem 4, which establishes the $(\mathcal{G}, \mathcal{R})$ -consistency of the *surrogate deferral loss* family.

Theorem 4 ($(\mathcal{G}, \mathcal{R})$ -consistency bounds). *Let $g \in \mathcal{G}$ be a multi-task model. Suppose there exists a non-decreasing function $\Gamma^\nu : \mathbb{R}^+ \rightarrow \mathbb{R}^+$ for $\nu \geq 0$, such that the \mathcal{R} -consistency bounds hold for any distribution \mathcal{D} :*

$$\begin{aligned} \mathcal{E}_{\Phi_{01}^\nu}(r) - \mathcal{E}_{\Phi_{01}^\nu}^*(\mathcal{R}) + \mathcal{U}_{\Phi_{01}^\nu}(\mathcal{R}) &\geq \\ \Gamma^\nu(\mathcal{E}_{\ell_{01}}(r) - \mathcal{E}_{\ell_{01}}^B(\mathcal{R}) + \mathcal{U}_{\ell_{01}}(\mathcal{R})), \end{aligned}$$

then for any $(g, r) \in \mathcal{G} \times \mathcal{R}$, any distribution \mathcal{D} and any $x \in \mathcal{X}$,

$$\begin{aligned} \mathcal{E}_{\ell_{\text{def}}}(g, r) - \mathcal{E}_{\ell_{\text{def}}}^B(\mathcal{G}, \mathcal{R}) + \mathcal{U}_{\ell_{\text{def}}}(\mathcal{G}, \mathcal{R}) &\leq \\ \bar{\Gamma}^\nu \left(\mathcal{E}_{\Phi_{\text{def}}^\nu}(r) - \mathcal{E}_{\Phi_{\text{def}}^\nu}^*(\mathcal{R}) + \mathcal{U}_{\Phi_{\text{def}}^\nu}(\mathcal{R}) \right) & \\ + \mathcal{E}_{c_0}(g) - \mathcal{E}_{c_0}^B(\mathcal{G}) + \mathcal{U}_{c_0}(\mathcal{G}), \end{aligned}$$

where $\bar{\Gamma}^\nu(u) = \|\bar{\tau}\|_1 \Gamma^\nu\left(\frac{u}{\|\bar{\tau}\|_1}\right)$, with $\Gamma^\nu(u) = \mathcal{T}^{-1, \nu}(u)$, and for the log-softmax surrogate, $\mathcal{T}^{\nu=1}(u) = \frac{1+u}{2} \log(1+u) + \frac{1-u}{2} \log(1-u)$.

The proof of Theorem 4, along with additional bounds for $\nu \geq 0$, is provided in Appendix C. Theorem 4 establishes sharper bounds than those in Mao et al. (2024e). Our bounds are specifically tailored for the cross-entropy surrogate family and explicitly depend on the parameter ν . Furthermore, the theorem shows that the tightness of these bounds is governed by the L_1 -norm of the aggregated costs, $\|\bar{\tau}\|_1$.

Moreover, we show that our surrogate losses are $(\mathcal{G}, \mathcal{R})$ -consistent for a *multiclass surrogate* family Φ_{01}^ν that is \mathcal{R} -consistent. Assuming $\mathcal{R} = \mathcal{R}_{\text{all}}$ and $\mathcal{G} = \mathcal{G}_{\text{all}}$, the minimizability gaps vanish, as demonstrated in [Steinwart \(2007\)](#). Therefore, by minimizing the *surrogates' deferral excess risk* while accounting for the minimizability gap, we establish that $\mathcal{E}_{\Phi_{\text{def}}^\nu}(r_k) - \mathcal{E}_{\Phi_{\text{def}}^\nu}^*(\mathcal{R}_{\text{all}}) + \mathcal{U}_{\Phi_{\text{def}}^\nu}(\mathcal{R}_{\text{all}}) \xrightarrow{k \rightarrow \infty} 0$. Since the multi-task model g is trained offline, it is reasonable to assume that the c_0 -excess risk satisfies $\mathcal{E}_{c_0}(g_k) - \mathcal{E}_{c_0}^B(\mathcal{G}_{\text{all}}) + \mathcal{U}_{c_0}(\mathcal{G}_{\text{all}}) \xrightarrow{k \rightarrow \infty} 0$. This result implies that the left-hand side is bounded above by zero, leading to $\mathcal{E}_{\ell_{\text{def}}}(g, r_k) - \mathcal{E}_{\ell_{\text{def}}}^B(\mathcal{G}_{\text{all}}, \mathcal{R}_{\text{all}}) + \mathcal{U}_{\ell_{\text{def}}}(\mathcal{G}_{\text{all}}, \mathcal{R}_{\text{all}}) \xrightarrow{k \rightarrow \infty} 0$, by leveraging the properties of $\bar{\Gamma}^\nu$. Consequently, the following corollary holds:

Corollary 5 (Bayes-consistency of the deferral surrogate losses). *Under the conditions of Theorem 4, assuming $(\mathcal{G}, \mathcal{R}) = (\mathcal{G}_{\text{all}}, \mathcal{R}_{\text{all}})$ and $\mathcal{E}_{c_0}(g_k) - \mathcal{E}_{c_0}^B(\mathcal{G}_{\text{all}}) \xrightarrow{k \rightarrow \infty} 0$, the surrogate deferral loss family Φ_{def}^ν is Bayes-consistent with respect to the true deferral loss ℓ_{def} . Specifically, minimizing the surrogates' deferral excess risk ensures the convergence of the true deferral excess risk. Formally, for $\{r_k\}_{k \in \mathbb{N}} \subset \mathcal{R}$ and $\{g_k\}_{k \in \mathbb{N}} \subset \mathcal{G}$:*

$$\begin{aligned} \mathcal{E}_{\Phi_{\text{def}}^\nu}(r_k) - \mathcal{E}_{\Phi_{\text{def}}^\nu}^*(\mathcal{R}_{\text{all}}) &\xrightarrow{k \rightarrow \infty} 0 \\ \implies \mathcal{E}_{\ell_{\text{def}}}(g_k, r_k) - \mathcal{E}_{\ell_{\text{def}}}^B(\mathcal{G}_{\text{all}}, \mathcal{R}_{\text{all}}) &\xrightarrow{k \rightarrow \infty} 0. \end{aligned} \tag{5}$$

This result demonstrates that as $k \rightarrow \infty$, the surrogates Φ_{def}^ν achieve asymptotic Bayes optimality for both the multi-task model g and the rejector r , effectively bridging the theoretical gap between the surrogate losses and the true deferral loss. Moreover, the pointwise optimal rejector $r^*(x)$ converges to a close approximation of the pointwise Bayes-optimal rejector $r^B(x)$, yielding a deferral rule consistent with the structure described in Lemma 2 ([Bartlett et al., 2006](#)).

Analysis of the minimizability gap: As shown by [Awasthi et al. \(2022\)](#), the minimizability gap does not vanish in general. Understanding its conditions, quantifying its magnitude, and identifying mitigation strategies are essential to ensuring that surrogate-based optimization aligns with task-specific objectives.

We provide a strong and novel characterization of the minimizability gap in the two-stage setting with multiple experts, extending the results of [Mao et al. \(2024f\)](#), who analyzed the gap in the context of learning with abstention (constant cost) for a single expert and a specific distribution.

Theorem 6 (Characterization Minimizability Gaps). *Assume \mathcal{R} symmetric and complete. Then, for the cross-entropy multiclass surrogates Φ_{01}^ν and any distribution \mathcal{D} , it follows for $\nu \geq 0$:*

$$\mathcal{C}_{\Phi_{\text{def}}^\nu}^{\nu,*} = \begin{cases} \|\bar{\tau}\|_1 H\left(\frac{\bar{\tau}}{\|\bar{\tau}\|_1}\right) & \nu = 1 \\ \|\bar{\tau}\|_1 - \|\bar{\tau}\|_\infty & \nu = 2 \\ \frac{1}{\nu-1} \left[\|\bar{\tau}\|_1 - \|\bar{\tau}\|_{\frac{1}{2-\nu}} \right] & \nu \in (1, 2) \\ \frac{1}{1-\nu} \left[\left(\sum_{k=0}^J \bar{\tau}_k^{\frac{1}{2-\nu}} \right)^{2-\nu} - \|\bar{\tau}\|_1 \right] & \text{otherwise,} \end{cases}$$

then the minimizability gap is,

$$\mathcal{U}_{\Phi_{\text{def}}^\nu}(\mathcal{R}) = \mathcal{E}_{\Phi_{\text{def}}^\nu}^*(\mathcal{R}) - \mathbb{E}_x[\inf_{r \in \mathcal{R}} \mathcal{C}_{\Phi_{\text{def}}^\nu}^\nu(r, x)]$$

with $\bar{\tau} = \{\mathbb{E}_{y,t|x}[\bar{\tau}_0], \dots, \mathbb{E}_{y,t|x}[\bar{\tau}_J]\}$, the aggregated costs $\tau_j = \sum_{k=0}^J c_k 1_{k \neq j}$, and the Shannon Entropy H .

We provide the proof in Appendix D. Theorem 6 characterizes the minimizability gap $\mathcal{U}_{\Phi_{\text{def}}^\nu}(\mathcal{R})$ for cross-entropy *multiclass surrogates* over symmetric and complete hypothesis sets \mathcal{R} . The gap varies with $\nu \geq 0$, exhibiting distinct behaviors across different surrogate. For $\nu = 1$, the gap is proportional to the Shannon entropy of the normalized expected cost vector $\frac{\bar{\tau}}{\|\bar{\tau}\|_1}$, increasing with entropy and reflecting higher uncertainty in misclassification distribution. At $\nu = 2$, it simplifies to the difference between the L_1 -norm and L_∞ -norm of $\bar{\tau}$, where a smaller gap indicates concentrated misclassifications, reducing uncertainty. For $\nu \in (1, 2)$, the gap balances the entropy-based sensitivity at $\nu = 1$ and the margin-based sensitivity at $\nu = 2$. As $\nu \rightarrow 1^+$, it emphasizes agents with higher misclassification counts; as $\nu \rightarrow 2^-$, it shifts toward aggregate misclassification counts. For $\nu < 1$, where $p = \frac{1}{2-\nu} \in (0, 1)$, the gap is more sensitive to misclassification distribution, increasing when errors are dispersed. For $\nu > 2$, where $p < 0$, reciprocal weighting reduces sensitivity to dominant errors, potentially decreasing the gap but at the risk of underemphasizing critical misclassifications.

In the setting of learning with abstention and a single expert ($J = 1$), assigning costs $\tau_0 = 1$ and $\tau_J = 1 - c$ recovers the minimizability gap introduced in (Mao et al., 2024f). Thus, our minimizability gap can be seen as a generalization to multiple experts, non-constant costs, and to any distribution \mathcal{D} .

4.3 Generalization Bound

We aim to quantify the generalization capability of our system, considering both the complexity of the hypothesis space and the quality of the participating agents. To this end, we define the empirical optimal rejector \hat{r}^B as the minimizer of the empirical generalization error:

$$\hat{r}^B = \arg \min_{r \in \mathcal{R}} \frac{1}{K} \sum_{k=1}^K \ell_{\text{def}}(g, m, r, z_k), \quad (6)$$

where ℓ_{def} denotes the *true deferral loss* function. To characterize the system's generalization ability, we utilize the Rademacher complexity, which measures the expressive richness of a hypothesis class by evaluating its capacity to fit random noise (Bartlett and Mendelson, 2003; Mohri et al., 2012). The proof of Lemma 7 is provided in Appendix E.

Lemma 7. *Let \mathcal{L}_1 be a family of functions mapping \mathcal{X} to $[0, 1]$, and let \mathcal{L}_2 be a family of functions mapping \mathcal{X} to $\{0, 1\}$. Define $\mathcal{L} = \{l_1 l_2 : l_1 \in \mathcal{L}_1, l_2 \in \mathcal{L}_2\}$. Then, the empirical Rademacher complexity of \mathcal{L} for any sample S of size K is bounded by:*

$$\hat{\mathfrak{R}}_S(\mathcal{L}) \leq \hat{\mathfrak{R}}_S(\mathcal{L}_1) + \hat{\mathfrak{R}}_S(\mathcal{L}_2). \quad (7)$$

For simplicity, we assume costs $c_0(g(x), z) = \ell_{01}(h(x), y) + \ell_{\text{reg}}(f(x), t)$ and $c_{j>0}(m_j(x), z) = c_0(m_j(x), z)$. We assume the regression loss ℓ_{reg} to be non-negative, bounded by L , and

Lipschitz. Furthermore, we assume that $m_{k,j}^h$ is drawn from the conditional distribution of the random variable M_j^h given parameters $\{X = x_k, Y = y_k\}$, and that $m_{k,j}^f$ is drawn from the conditional distribution of M_j^f given $\{X = x_k, T = t_k\}$. We define the family of deferral loss functions as $\mathcal{L}_{\text{def}} = \{\ell_{\text{def}} : \mathcal{G} \times \mathcal{R} \times \mathcal{M} \times \mathcal{Z} \rightarrow [0, 1]\}$. Under these assumptions, we derive the generalization bounds for the binary setting as follows:

Theorem 8 (Learning bounds of the deferral loss). *For any expert M_j , any distribution \mathcal{D} over \mathcal{Z} , we have with probability $1 - \delta$ for $\delta \in [0, 1/2]$, that the following bound holds at the optimum:*

$$\mathcal{E}_{\ell_{\text{def}}}(h, f, r) \leq \widehat{\mathcal{E}}_{\ell_{\text{def}}}(h, f, r) + 2\mathfrak{R}_K(\mathcal{L}_{\text{def}}) + \sqrt{\frac{\log 1/\delta}{2K}},$$

with

$$\begin{aligned} \mathfrak{R}_K(\mathcal{L}_{\text{def}}) &\leq \frac{1}{2}\mathfrak{R}_K(\mathcal{H}) + \mathfrak{R}_K(\mathcal{F}) + \sum_{j=1}^J \Omega(m_j^h, y) \\ &\quad + \left(\sum_{j=1}^J \max_t \ell_{\text{reg}}(m_j^f, t) + 2 \right) \mathfrak{R}_K(\mathcal{R}), \end{aligned}$$

with $\Omega(m_j^h, y) = \frac{1}{2}\mathcal{D}(m_j^h \neq y) \exp\left(-\frac{K}{8}\mathcal{D}(m_j^h \neq y)\right) + \mathcal{R}_{K\mathcal{D}(m_j^h \neq y)/2}(\mathcal{R})$.

We prove Theorem 8 in Appendix F. The terms $\mathfrak{R}_K(\mathcal{H})$ and $\mathfrak{R}_K(\mathcal{F})$ denote the Rademacher complexities of the hypothesis class \mathcal{H} and function class \mathcal{F} , respectively, indicating that the generalization bounds depend on the complexity of the pre-trained model. The term $\Omega(m_j^h, y)$ captures the impact of each expert’s classification error on the learning bound.

It includes an exponentially decaying factor, $\frac{\mathcal{D}(m_j^h \neq y)}{2} \exp\left(-\frac{K\mathcal{D}(m_j^h \neq y)}{8}\right)$, which decreases rapidly as the sample size K grows or as the expert’s error rate $\mathcal{D}(m_j^h \neq y)$ declines (Mozannar and Sontag, 2020). This reflects the intuition that more accurate experts contribute less to the bound, improving overall generalization. Finally, the last term suggests that the generalization properties of our *true deferral loss* depend on the expert’s regression performance.

5 Experiments

In this section, we present the performance improvements achieved by the proposed Learning-to-Defer surrogate in a multi-task context. Specifically, we demonstrate that our approach excels in object detection, a task where classification and regression components are inherently intertwined, and where existing L2D methods encounter significant limitations. Furthermore, we evaluate our approach on an Electronic Health Record task, jointly predicting mortality (classification) and length of stay (regression), comparing our results with Mao et al. (2023a, 2024e).

For each experiment, we report the mean and standard deviation across four independent trials to account for variability in the results. All training and evaluation were conducted on an NVIDIA H100 GPU. We give our training algorithm in Appendix A. Additional figures and details are provided in Appendix G. To ensure reproducibility, we have made our implementation publicly available.

5.1 Object Detection Task

We evaluate our approach using the Pascal VOC dataset (Everingham et al., 2010), a multi-object detection benchmark. This is the first time such a multi-task problem has been explored within the L2D framework as previous L2D approaches require the classification and regression component to be independent (Mao et al., 2023a, 2024e).

Dataset and Metrics: The PASCAL Visual Object Classes (VOC) dataset (Everingham et al., 2010) serves as a widely recognized benchmark in computer vision for evaluating object detection models. It consists of annotated images spanning 20 object categories, showcasing diverse scenes with varying scales, occlusions, and lighting conditions. To assess object detection performance, we report the mean Average Precision (mAP), a standard metric in the field. The mAP quantifies the average precision across all object classes by calculating the area under the precision-recall curve for each class. Additionally, in the context of L2D, we report the allocation metric (All.), which represents the ratio of allocated queries per agent.

Agents setting: We trained three distinct Faster R-CNN models (Ren et al., 2016) to serve as our agents, differentiated by their computational complexities. The smallest, characterized by GFLOPS = 12.2, represents our model $g \in \mathcal{G}$ with $\mathcal{G} = \{g : g(x) = (h \circ w(x), f \circ w(x)) \mid w \in \mathcal{W}, h \in \mathcal{H}, f \in \mathcal{F}\}$. The medium-sized, denoted as Expert 1, has a computational cost of GFLOPS = 134.4, while the largest, Expert 2, operates at GFLOPS = 280.3. To account for the difference in complexity between Experts 1 and 2, we define the ratio $R_G = 280.3/134.4$ and set the query cost for Expert 1 as $\beta_1 = \beta_2/R_G$. This parameterization reflects the relative computational costs of querying experts. We define the agent costs as $c_0(g(x), z) = \text{mAP}(g(x), z)$ and $c_{j \in [J]}(m_j(x), z) = \text{mAP}(m_j(x), z)$. We report the performance metrics of the agents alongside additional training details in Appendix G.1.

Rejector: The rejector is trained using a smaller version of the Faster R-CNN model (Ren et al., 2016). Training is performed for 200 epochs using the Adam optimizer (Kingma and Ba, 2017) with a learning rate of 0.001 and a batch size of 64. The checkpoint achieving the lowest empirical risk on the validation set is selected for evaluation.

Results: In Figure 5.1, we observe that for lower cost values, specifically when $\beta_1 < 0.15$, the system consistently avoids selecting Expert 1. This outcome arises because the cost difference between β_1 and β_2 is negligible, making it more advantageous to defer to Expert 2 (the most accurate expert), where the modest cost increase is offset by superior outcomes. When $\beta_2 = 0.15$, however, it becomes optimal to defer to both experts and model at the same time. In particular, there exist instances $x \in \mathcal{X}$ where both Expert 1 and Expert 2 correctly predict the target (while the model does not). In such cases, Expert 1 is preferred due to its lower cost $\beta_1 < \beta_2$. Conversely, for instances $x \in \mathcal{X}$ where Expert 2 is accurate and Expert 1 (along with the model) is incorrect, the system continues to select Expert 2, as β_2 remains relatively low. For $\beta_2 \geq 0.2$, the increasing cost differential between the experts shifts the balance in favor of Expert 1, enabling the system to achieve strong performance while minimizing overall costs.

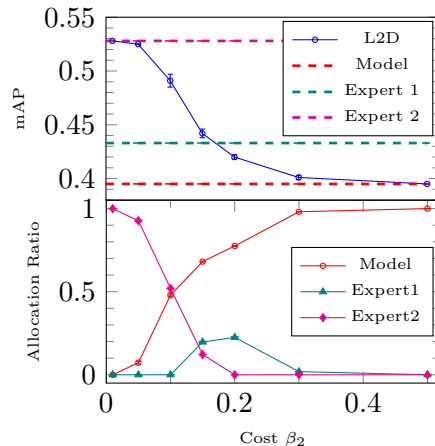


Figure 1: Performance comparison across different cost values β_2 on Pascal VOC (Everingham et al., 2010). The table reports the mean Average Precision (mAP) and the allocation ratio for the model and two experts with mean and variance. We report these results in Appendix Table 3.

This demonstrates that our approach effectively allocates queries among agents, thereby enhancing the overall performance of the system, even when the classification and regression tasks are interdependent.

5.2 EHR Task

We compare our novel approach against existing two-stage L2D methods (Mao et al., 2023a, 2024e). Unlike the first experiment on object detection (Subsection 5.1), where classification and regression tasks are interdependent, this evaluation focuses on a second scenario where the two tasks can be treated independently.

Dataset and Metrics: The Medical Information Mart for Intensive Care IV (MIMIC-IV) dataset (Johnson et al., 2023) is a comprehensive collection of de-identified health-related data patients admitted to critical care units. For our analysis, we focus on two tasks: mortality prediction and length-of-stay prediction, corresponding to classification and regression tasks, respectively. To evaluate performance, we report accuracy (Acc) for the mortality prediction task, which quantifies classification performance, and Smooth L1 loss (sL1) for the length-of-stay prediction task, which measures the deviation between the predicted and actual values. Additionally, we report the allocation metric (All.) for L2D to capture query allocation behavior.

Agents setting: We consider two experts, M_1 and M_2 , acting as specialized agents, aligning with the category allocation described in (Mozannar and Sontag, 2020; Verma et al., 2022; Verma and Nalisnick, 2022; Cao et al., 2024). The dataset is partitioned into $Z = 6$ clusters using the K -means algorithm (Lloyd, 1982), where Z is selected via the Elbow method (Thorndike, 1953). The clusters are denoted as $\{C_1, C_2, \dots, C_Z\}$. Each cluster rep-

resents a subset of data instances grouped by feature similarity, enabling features-specific specialization by the experts. The experts are assumed to specialize in distinct subsets of clusters based on the task. For classification, M_1 correctly predicts the outcomes for clusters $C_{\text{cla}}^{M_1} = \{C_1, C_2, C_4\}$, while M_2 handles clusters $C_{\text{cla}}^{M_2} = \{C_1, C_5, C_6\}$. Notably, cluster C_1 is shared between the two experts, reflecting practical scenarios where domain knowledge overlaps. For regression tasks, M_1 is accurate on clusters $C_{\text{reg}}^{M_1} = \{C_1, C_3, C_5\}$, while M_2 specializes in clusters $C_{\text{reg}}^{M_2} = \{C_1, C_4, C_6\}$. Here too, overlap is modeled, with cluster C_1 being common to both experts and classification-regression task. Note that the category assignments do not follow any specific rule.

We assume that each expert produces correct predictions for the clusters they are assigned (Verma et al., 2022; Mozannar and Sontag, 2020). Conversely, for clusters outside their expertise, predictions are assumed to be incorrect. In such cases, for length-of-stay predictions, the outcomes are modeled using a uniform probability distribution to reflect uncertainty. The detailed performance evaluation of these agents is provided in Appendix G.2.

The model utilizes two compact transformer architectures (Vaswani et al., 2017) for addressing both classification and regression tasks, formally defined as $\mathcal{G} = \{g : g(x) = (h(x), f(x)) \mid h \in \mathcal{H}, f \in \mathcal{F}\}$. The agent’s costs are specified as $c_0(g(x), z) = \lambda^{\text{cla}} \ell_{01}(h(x), y) + \lambda^{\text{reg}} \ell_{\text{reg}}(f(x), t)$ and $c_{j \in [J]}(m_j(x), z) = c_0(m_j(x), z) + \beta_j$. Consistent with prior works (Mozannar and Sontag, 2020; Verma et al., 2022; Mao et al., 2023a, 2024e), we set $\beta_j = 0$.

Rejectors: The two-stage L2D rejectors are trained using a small transformer model (Vaswani et al., 2017) as the encoder, following the approach outlined by Yang et al. (2023), with a classification head for query allocation. Training is performed over 100 epochs with a learning rate of 0.003, a warm-up period of 0.1, a cosine learning rate scheduler, the Adam optimizer (Kingma and Ba, 2017), and a batch size of 1024 for all baselines. The checkpoint with the lowest empirical risk on the validation set is selected for evaluation.

Results: Table 5.2 compares the performance of our proposed Learning-to-Defer (Ours) approach with two existing methods: a classification-focused rejector (Mao et al., 2023a) and a regression-focused rejector (Mao et al., 2024e). The results highlight the limitations of task-specific rejectors and the advantages of our balanced approach.

Rejector	Acc (%)	sL1	All. Model	All. Expert 1	All. Expert 2
Mao et al. (2023a)	71.3 ± .1	1.45 ± .03	.60 ± .02	.01 ± .01	.39 ± .02
Mao et al. (2024e)	50.7 ± .8	1.18 ± .05	.38 ± .01	.37 ± .02	.25 ± .01
Ours	70.0 ± .5	1.28 ± .02	.66 ± .01	.12 ± .02	.22 ± .01

Table 1: Performance comparison of different two-stage L2D. The table reports accuracy (Acc), smooth L1 loss (sL1), and allocation rates (All.) to the model and experts with mean and variance.

The classification-focused rejector achieves the highest classification accuracy at 71.3% but struggles with regression, as reflected by its high smooth L1 loss of 1.45. On the other hand, the regression-focused rejector achieves the best regression performance with an sL1 loss of 1.18 but performs poorly in classification with an accuracy of 50.7%. In contrast, our method balances performance across tasks, achieving a classification accuracy of 70.0% and

an sL1 loss of 1.28. Moreover, it significantly reduces reliance on experts, allocating 66% of queries to the model compared to 60% for Mao et al. (2023a) and 38% for Mao et al. (2024e). Expert involvement is minimized, with only 12% and 22% of queries allocated to Experts 1 and 2, respectively.

Since the experts possess distinct knowledge for the two tasks ($C_{\text{cla}}^{M_1}$ and $C_{\text{reg}}^{M_1}$ for M_1), independently deferring classification and regression may lead to suboptimal performance. In contrast, our approach models deferral decisions dependently, considering the interplay between the two components to achieve better overall results.

6 Conclusion

We introduced a Two-Stage Learning-to-Defer framework for multi-task problems, extending existing approaches to jointly handle classification and regression. We proposed a two-stage surrogate loss family that is both $(\mathcal{G}, \mathcal{R})$ -consistent and Bayes-consistent for any cross-entropy-based surrogate. Additionally, we derived tight consistency bounds linked to cross-entropy losses and the L_1 -norm of aggregated costs. We further established novel minimizability gap for the two-stage setting, generalizing prior results to Learning-to-Defer with multiple experts. Finally, we showed that our learning bounds improve with a richer hypothesis space and more confident experts.

We validated our framework on two challenging tasks: (i) object detection, where classification and regression are inherently interdependent—beyond the scope of existing L2D methods; and (ii) electronic health record analysis, where we demonstrated that current L2D approaches can be suboptimal even when classification and regression tasks are independent.

REFERENCES

- Pranjal Awasthi, Anqi Mao, Mehryar Mohri, and Yutao Zhong. Multi-class h-consistency bounds. In *Proceedings of the 36th International Conference on Neural Information Processing Systems, NIPS '22*, Red Hook, NY, USA, 2022. Curran Associates Inc. ISBN 9781713871088.
- Yoganand Balagurunathan, Ross Mitchell, and Issam El Naqa. Requirements and reliability of AI in the medical context. *Physica Medica*, 83:72–78, 2021.
- Peter Bartlett, Michael Jordan, and Jon McAuliffe. Convexity, classification, and risk bounds. *Journal of the American Statistical Association*, 101:138–156, 02 2006. doi: 10.1198/016214505000000907.
- Peter L. Bartlett and Shahar Mendelson. Rademacher and Gaussian complexities: Risk bounds and structural results. *J. Mach. Learn. Res.*, 3(null):463–482, March 2003. ISSN 1532-4435.
- Peter L. Bartlett and Marten H. Wegkamp. Classification with a reject option using a hinge loss. *The Journal of Machine Learning Research*, 9:1823–1840, June 2008.
- Nina L Corvelo Benz and Manuel Gomez Rodriguez. Counterfactual inference of second opinions. In *Uncertainty in Artificial Intelligence*, pages 453–463. PMLR, 2022.

- Joseph Berkson. Application of the logistic function to bio-assay. *Journal of the American Statistical Association*, 39:357–365, 1944. URL <https://api.semanticscholar.org/CorpusID:122893121>.
- Shyamal Buch, Victor Escorcia, Chuanqi Shen, Bernard Ghanem, and Juan Carlos Niebles. SST: Single-stream temporal action proposals. In *Proceedings of the IEEE Conference on Computer Vision and Pattern Recognition*, pages 2911–2920, 2017.
- Yuzhou Cao, Tianchi Cai, Lei Feng, Lihong Gu, Jinjie Gu, Bo An, Gang Niu, and Masashi Sugiyama. Generalizing consistent multi-class classification with rejection to be compatible with arbitrary losses. In *Proceedings of the 36th International Conference on Neural Information Processing Systems*, NIPS ’22, Red Hook, NY, USA, 2022. Curran Associates Inc. ISBN 9781713871088.
- Yuzhou Cao, Hussein Mozannar, Lei Feng, Hongxin Wei, and Bo An. In defense of softmax parametrization for calibrated and consistent learning to defer. In *Proceedings of the 37th International Conference on Neural Information Processing Systems*, NIPS ’23, Red Hook, NY, USA, 2024. Curran Associates Inc.
- Nicolas Carion, Francisco Massa, Gabriel Synnaeve, Nicolas Usunier, Alexander Kirillov, and Sergey Zagoruyko. End-to-end object detection with transformers. In *Computer Vision – ECCV 2020: 16th European Conference, Glasgow, UK, August 23–28, 2020, Proceedings, Part I*, page 213–229, Berlin, Heidelberg, 2020. Springer-Verlag. ISBN 978-3-030-58451-1. doi: 10.1007/978-3-030-58452-8_13. URL https://doi.org/10.1007/978-3-030-58452-8_13.
- Mohammad-Amin Charusaie, Hussein Mozannar, David Sontag, and Samira Samadi. Sample efficient learning of predictors that complement humans. In *International Conference on Machine Learning*, pages 2972–3005. PMLR, 2022.
- C. Chow. On optimum recognition error and reject tradeoff. *IEEE Transactions on Information Theory*, 16(1):41–46, January 1970. doi: 10.1109/TIT.1970.1054406.
- Corinna Cortes and Vladimir Naumovich Vapnik. Support-vector networks. *Machine Learning*, 20:273–297, 1995. URL <https://api.semanticscholar.org/CorpusID:52874011>.
- Corinna Cortes, Giulia DeSalvo, and Mehryar Mohri. Learning with rejection. In *Algorithmic Learning Theory: 27th International Conference, ALT 2016, Bari, Italy, October 19–21, 2016, Proceedings 27*, pages 67–82. Springer, 2016.
- Mark Everingham, Luc Gool, Christopher K. Williams, John Winn, and Andrew Zisserman. The pascal visual object classes (voc) challenge. *Int. J. Comput. Vision*, 88(2):303–338, June 2010. ISSN 0920-5691. doi: 10.1007/s11263-009-0275-4. URL <https://doi.org/10.1007/s11263-009-0275-4>.
- Yonatan Geifman and Ran El-Yaniv. Selective classification for deep neural networks. In I. Guyon, U. Von Luxburg, S. Bengio, H. Wallach, R. Fergus, S. Vishwanathan, and R. Garnett, editors, *Advances in Neural Information Processing Systems*, volume 30. Curran Associates, Inc., 2017. URL https://proceedings.neurips.cc/paper_files/paper/2017/file/4a8423d5e91fda00bb7e46540e2b0c.

Aritra Ghosh, Himanshu Kumar, and P. Shanti Sastry. Robust loss functions under label noise for deep neural networks. *ArXiv*, abs/1712.09482, 2017. URL <https://api.semanticscholar.org/CorpusID:6546734>.

R Girshick. Fast R-CNN. *arXiv preprint arXiv:1504.08083*, 2015.

Patrick Hemmer, Max Schemmer, Michael Vössing, and Niklas Kühl. Human-AI complementarity in hybrid intelligence systems: A structured literature review. *PACIS*, page 78, 2021.

Patrick Hemmer, Sebastian Schellhammer, Michael Vössing, Johannes Jakubik, and Gerhard Satzger. Forming effective human-AI teams: Building machine learning models that complement the capabilities of multiple experts. In Lud De Raedt, editor, *Proceedings of the Thirty-First International Joint Conference on Artificial Intelligence, IJCAI-22*, pages 2478–2484. International Joint Conferences on Artificial Intelligence Organization, 7 2022. doi: 10.24963/ijcai.2022/344. URL <https://doi.org/10.24963/ijcai.2022/344>. Main Track.

Alistair EW Johnson, Tom J Pollard, Lu Shen, Li-wei H Lehman, Mengling Feng, Mohammad Ghassemi, Benjamin Moody, Peter Szolovits, Leo Anthony Celi, and Roger G Mark. MIMIC-III, a freely accessible critical care database. *Scientific data*, 3(1):1–9, 2016.

Alistair EW Johnson, Lucas Bulgarelli, Lu Shen, Alvin Gayles, Ayad Shammout, Steven Horng, Tom J Pollard, Sicheng Hao, Benjamin Moody, Brian Gow, et al. MIMIC-IV, a freely accessible electronic health record dataset. *Scientific data*, 10(1):1, 2023.

Gavin Kerrigan, Padhraic Smyth, and Mark Steyvers. Combining human predictions with model probabilities via confusion matrices and calibration. In M. Ranzato, A. Beygelzimer, Y. Dauphin, P.S. Liang, and J. Wortman Vaughan, editors, *Advances in Neural Information Processing Systems*, volume 34, pages 4421–4434. Curran Associates, Inc., 2021. URL https://proceedings.neurips.cc/paper_files/paper/2021/file/234b941e88b755b7a72a1c1dd5022f

Vijay Keswani, Matthew Lease, and Krishnaram Kenthapadi. Towards unbiased and accurate deferral to multiple experts. In *Proceedings of the 2021 AAAI/ACM Conference on AI, Ethics, and Society*, AIES '21, page 154–165, New York, NY, USA, 2021. Association for Computing Machinery. ISBN 9781450384735. doi: 10.1145/3461702.3462516. URL <https://doi.org/10.1145/3461702.3462516>.

Diederik P. Kingma and Jimmy Ba. Adam: A method for stochastic optimization, 2017. URL <https://arxiv.org/abs/1412.6980>.

Shuqi Liu, Yuzhou Cao, Qiaozhen Zhang, Lei Feng, and Bo An. Mitigating underfitting in learning to defer with consistent losses. In *International Conference on Artificial Intelligence and Statistics*, pages 4816–4824. PMLR, 2024.

S. Lloyd. Least squares quantization in PCM. *IEEE Transactions on Information Theory*, 28(2):129–137, 1982. doi: 10.1109/TIT.1982.1056489.

- Phil Long and Rocco Servedio. Consistency versus realizable h -consistency for multiclass classification. In Sanjoy Dasgupta and David McAllester, editors, *Proceedings of the 30th International Conference on Machine Learning*, number 3 in Proceedings of Machine Learning Research, pages 801–809, Atlanta, Georgia, USA, 17–19 Jun 2013. PMLR. URL <https://proceedings.mlr.press/v28/long13.html>.
- David Madras, Toniann Pitassi, and Richard Zemel. Predict responsibly: Improving fairness and accuracy by learning to defer. In *Proceedings of the 32nd International Conference on Neural Information Processing Systems, NIPS’18*, page 6150–6160, 2018.
- Anqi Mao, Christopher Mohri, Mehryar Mohri, and Yutao Zhong. Two-stage learning to defer with multiple experts. In *Thirty-seventh Conference on Neural Information Processing Systems, 2023a*. URL <https://openreview.net/forum?id=GI1sHOT4b2>.
- Anqi Mao, Mehryar Mohri, and Yutao Zhong. Cross-entropy loss functions: Theoretical analysis and applications. In *Proceedings of the 40th International Conference on Machine Learning, ICML’23, 2023b*.
- Anqi Mao, Mehryar Mohri, and Yutao Zhong. Predictor-rejector multi-class abstention: Theoretical analysis and algorithms. In *International Conference on Algorithmic Learning Theory*, pages 822–867. PMLR, 2024a.
- Anqi Mao, Mehryar Mohri, and Yutao Zhong. Enhanced h -consistency bounds. *arXiv preprint arXiv:2407.13722*, 2024b.
- Anqi Mao, Mehryar Mohri, and Yutao Zhong. Principled approaches for learning to defer with multiple experts. In *International Workshop on Combinatorial Image Analysis*, pages 107–135. Springer, 2024c.
- Anqi Mao, Mehryar Mohri, and Yutao Zhong. Realizable h -consistent and bayes-consistent loss functions for learning to defer, 2024d. URL <https://arxiv.org/abs/2407.13732>.
- Anqi Mao, Mehryar Mohri, and Yutao Zhong. Regression with multi-expert deferral. *arXiv 2403.19494*, 2024e. <https://arxiv.org/abs/2403.19494>.
- Anqi Mao, Mehryar Mohri, and Yutao Zhong. Theoretically grounded loss functions and algorithms for score-based multi-class abstention. In *International Conference on Artificial Intelligence and Statistics*, pages 4753–4761. PMLR, 2024f.
- Mehryar Mohri, Afshin Rostamizadeh, and Ameet Talwalkar. *Foundations of Machine Learning*. The MIT Press, 2012. ISBN 026201825X.
- Yannis Montreuil, Axel Carlier, Lai Xing Ng, and Wei Tsang Ooi. Learning-to-defer for extractive question answering, 2024. URL <https://arxiv.org/abs/2410.15761>.
- Hussein Mozannar and David Sontag. Consistent estimators for learning to defer to an expert. In *Proceedings of the 37th International Conference on Machine Learning, ICML’20, 2020*.

Hussein Mozannar, Hunter Lang, Dennis Wei, Prasanna Sattigeri, Subhro Das, and David A. Sontag. Who should predict? exact algorithms for learning to defer to humans. In *International Conference on Artificial Intelligence and Statistics*, 2023. URL <https://api.semanticscholar.org/CorpusID:255941521>.

Harish G. Ramaswamy, Ambuj Tewari, and Shivani Agarwal. Consistent algorithms for multiclass classification with an abstain option. *Electronic Journal of Statistics*, 12(1):530–554, 2018. doi: 10.1214/17-EJS1388. URL <https://doi.org/10.1214/17-EJS1388>.

Joseph Redmon, Santosh Divvala, Ross Girshick, and Ali Farhadi. You only look once: Unified, real-time object detection. In *2016 IEEE Conference on Computer Vision and Pattern Recognition (CVPR)*, pages 779–788, 2016.

Shaoqing Ren, Kaiming He, Ross Girshick, and Jian Sun. Faster r-cnn: Towards real-time object detection with region proposal networks, 2016. URL <https://arxiv.org/abs/1506.01497>.

Ingo Steinwart. How to compare different loss functions and their risks. *Constructive Approximation*, 26:225–287, 2007. URL <https://api.semanticscholar.org/CorpusID:16660598>.

Dharmesh Tailor, Aditya Patra, Rajeev Verma, Putra Manggala, and Eric Nalisnick. Learning to defer to a population: A meta-learning approach. In Sanjoy Dasgupta, Stephan Mandt, and Yingzhen Li, editors, *Proceedings of The 27th International Conference on Artificial Intelligence and Statistics*, volume 238 of *Proceedings of Machine Learning Research*, pages 3475–3483. PMLR, 02–04 May 2024. URL <https://proceedings.mlr.press/v238/tailor24a.html>.

Ambuj Tewari and Peter L. Bartlett. On the consistency of multiclass classification methods. *Journal of Machine Learning Research*, 8(36):1007–1025, 2007. URL <http://jmlr.org/papers/v8/tewari07a.html>.

Robert L. Thorndike. Who belongs in the family? *Psychometrika*, 18:267–276, 1953. URL <https://api.semanticscholar.org/CorpusID:120467216>.

Ashish Vaswani, Noam Shazeer, Niki Parmar, Jakob Uszkoreit, Llion Jones, Aidan N Gomez, Łukasz Kaiser, and Illia Polosukhin. Attention is all you need. In I. Guyon, U. Von Luxburg, S. Bengio, H. Wallach, R. Fergus, S. Vishwanathan, and R. Garnett, editors, *Advances in Neural Information Processing Systems*, volume 30. Curran Associates, Inc., 2017. URL https://proceedings.neurips.cc/paper_files/paper/2017/file/3f5ee243547dee91fbd053c1c4a845

Rajeev Verma and Eric Nalisnick. Calibrated learning to defer with one-vs-all classifiers. In *International Conference on Machine Learning*, pages 22184–22202. PMLR, 2022.

Rajeev Verma, Daniel Barrejon, and Eric Nalisnick. Learning to defer to multiple experts: Consistent surrogate losses, confidence calibration, and conformal ensembles. In *International Conference on Artificial Intelligence and Statistics*, 2022. URL <https://api.semanticscholar.org/CorpusID:253237048>.

Chaoqi Yang, Zhenbang Wu, Patrick Jiang, Zhen Lin, Junyi Gao, Benjamin Danek, and Jimeng Sun. PyHealth: A deep learning toolkit for healthcare predictive modeling. In *Proceedings of the 27th ACM SIGKDD International Conference on Knowledge Discovery and Data Mining (KDD) 2023*, 2023. URL <https://github.com/sunlabuiuc/PyHealth>.

Mingyuan Zhang and Shivani Agarwal. Bayes consistency vs. h-consistency: The interplay between surrogate loss functions and the scoring function class. In H. Larochelle, M. Ranzato, R. Hadsell, M.F. Balcan, and H. Lin, editors, *Advances in Neural Information Processing Systems*, volume 33, pages 16927–16936. Curran Associates, Inc., 2020. URL https://proceedings.neurips.cc/paper_files/paper/2020/file/c4c28b367e14df88993ad475dedf6b

Tong Zhang. Statistical behavior and consistency of classification methods based on convex risk minimization. *Annals of Statistics*, 32, 12 2002. doi: 10.1214/aos/1079120130.

Appendix A. Algorithm

Algorithm 1 Two-Stage Learning-to-Defer for Multi-Task Learning Algorithm

Input: Dataset $\{(x_k, y_k, t_k)\}_{k=1}^K$, multi-task model $g \in \mathcal{G}$, experts $m \in \mathcal{M}$, rejector $r \in \mathcal{R}$, number of epochs EPOCH, batch size B , learning rate η .

Initialization: Initialize rejector parameters θ .

for $i = 1$ to EPOCH **do**

Shuffle dataset $\{(x_k, y_k, t_k)\}_{k=1}^K$.

for each mini-batch $\mathcal{B} \subset \{(x_k, y_k, t_k)\}_{k=1}^K$ of size B **do**

Extract input-output pairs $z = (x, y, t) \in \mathcal{B}$.

Query model $g(x)$ and experts $m(x)$. {Agents are pre-trained and fixed}

Evaluate costs $c_0(g(x), z)$ and $c_{j>0}(m(x), z)$. {Compute task-specific costs}

Compute rejector prediction $r(x) = \arg \max_{j \in \mathcal{A}} r(x, j)$. {Rejector decision}

Compute surrogate deferral empirical risk $\hat{\mathcal{E}}_{\Phi_{\text{def}}}$:

$$\hat{\mathcal{E}}_{\Phi_{\text{def}}} = \frac{1}{B} \sum_{z \in \mathcal{B}} [\Phi_{\text{def}}(g, r, m, z)]. \quad \text{{Empirical risk computation}}$$

Update parameters θ using gradient descent:

$$\theta \leftarrow \theta - \eta \nabla_{\theta} \hat{\mathcal{E}}_{\Phi_{\text{def}}}. \quad \text{{Parameter update}}$$

end for

end for

Return: trained rejector model r^* .

We will prove key lemmas and theorems stated in our main paper.

Appendix B. Proof of Lemma 2

We aim to prove Lemma 2, which establishes the optimal deferral decision by minimizing the conditional risk.

By definition, the Bayes-optimal rejector $r^B(x)$ minimizes the conditional risk $\mathcal{C}_{\ell_{\text{def}}}$, given by:

$$\mathcal{C}_{\ell_{\text{def}}}(g, r, x) = \mathbb{E}_{y,t|x}[\ell_{\text{def}}(g, r, m, z)]. \quad (8)$$

Expanding the expectation, we obtain:

$$\mathcal{C}_{\ell_{\text{def}}}(g, r, x) = \mathbb{E}_{y,t|x} \left[\sum_{j=0}^J c_j(g(x), m_j(x), z) \mathbf{1}_{r(x)=j} \right]. \quad (9)$$

Using the linearity of expectation, this simplifies to:

$$\mathcal{C}_{\ell_{\text{def}}}(g, r, x) = \sum_{j=0}^J \mathbb{E}_{y,t|x} [c_j(g(x), m_j(x), z)] \mathbf{1}_{r(x)=j}. \quad (10)$$

Since we seek the rejector that minimizes the expected loss, the Bayes-conditional risk is given by:

$$\mathcal{C}_{\ell_{\text{def}}}^B(g, r, x) = \inf_{g \in \mathcal{G}, r \in \mathcal{R}} \mathbb{E}_{y,t|x}[\ell_{\text{def}}(g, r, m, z)]. \quad (11)$$

Rewriting this expression, we obtain:

$$\mathcal{C}_{\ell_{\text{def}}}^B(g, r, x) = \inf_{r \in \mathcal{R}} \mathbb{E}_{y, t|x} \left[\inf_{g \in \mathcal{G}} c_0(g(x), z) 1_{r(x)=0} + \sum_{j=1}^J c_j(m_j(x), z) 1_{r(x)=j} \right]. \quad (12)$$

This leads to the following minimization problem:

$$\mathcal{C}_{\ell_{\text{def}}}^B(g, r, x) = \min \left\{ \inf_{g \in \mathcal{G}} \mathbb{E}_{y, t|x} [c_0(g(x), z)], \min_{j \in [J]} \mathbb{E}_{y, t|x} [c_j(m_j(x), z)] \right\}. \quad (13)$$

To simplify notation, we define:

$$\bar{c}_j^* = \begin{cases} \inf_{g \in \mathcal{G}} \mathbb{E}_{y, t|x} [c_0(g(x), z)], & \text{if } j = 0, \\ \mathbb{E}_{y, t|x} [c_j(m_j(x), z)], & \text{otherwise.} \end{cases} \quad (14)$$

Thus, the Bayes-conditional risk simplifies to:

$$\mathcal{C}_{\ell_{\text{def}}}^B(g, r, x) = \min_{j \in \mathcal{A}} \bar{c}_j^*. \quad (15)$$

Since the rejector selects the decision with the lowest expected cost, the optimal rejector is given by:

$$r^B(x) = \begin{cases} 0, & \text{if } \inf_{g \in \mathcal{G}} \mathbb{E}_{y, t|x} [c_0(g(x), z)] \leq \min_{j \in [J]} \mathbb{E}_{y, t|x} [c_j(m_j(x), z)], \\ j, & \text{otherwise.} \end{cases} \quad (16)$$

This completes the proof. \square

Appendix C. Proof Theorem 4

Before proving the desired Theorem 4, we will use the following Lemma 9 (Awasthi et al., 2022; Mao et al., 2024e):

Lemma 9 (\mathcal{R} -consistency bound). *Assume that the following \mathcal{R} -consistency bounds holds for $r \in \mathcal{R}$, and any distribution*

$$\mathcal{E}_{\ell_{01}}(r) - \mathcal{E}_{\ell_{01}}^*(\mathcal{R}) + \mathcal{U}_{\ell_{01}}(\mathcal{R}) \leq \Gamma^\nu(\mathcal{E}_{\Phi_{01}^\nu}(r) - \mathcal{E}_{\Phi_{01}^\nu}^*(\mathcal{R}) + \mathcal{U}_{\Phi_{01}^\nu}(\mathcal{R}))$$

then for $p \in (p_0 \dots p_J) \in \Delta^{|\mathcal{A}|}$ and $x \in \mathcal{X}$, we get

$$\sum_{j=0}^J p_j 1_{r(x) \neq j} - \inf_{r \in \mathcal{R}} \sum_{j=0}^J p_j 1_{r(x) \neq j} \leq \Gamma^\nu \left(\sum_{j=0}^J p_j \Phi_{01}^\nu(r, x, j) - \inf_{r \in \mathcal{R}} \sum_{j=0}^J p_j \Phi_{01}^\nu(r, x, j) \right)$$

Theorem 4 ($(\mathcal{G}, \mathcal{R})$ -consistency bounds). *Let $g \in \mathcal{G}$ be a multi-task model. Suppose there exists a non-decreasing function $\Gamma^\nu : \mathbb{R}^+ \rightarrow \mathbb{R}^+$ for $\nu \geq 0$, such that the \mathcal{R} -consistency bounds hold for any distribution \mathcal{D} :*

$$\begin{aligned} \mathcal{E}_{\Phi_{01}^\nu}(r) - \mathcal{E}_{\Phi_{01}^\nu}^*(\mathcal{R}) + \mathcal{U}_{\Phi_{01}^\nu}(\mathcal{R}) &\geq \\ \Gamma^\nu(\mathcal{E}_{\ell_{01}}(r) - \mathcal{E}_{\ell_{01}}^B(\mathcal{R}) + \mathcal{U}_{\ell_{01}}(\mathcal{R})), & \end{aligned}$$

then for any $(g, r) \in \mathcal{G} \times \mathcal{R}$, any distribution \mathcal{D} and any $x \in \mathcal{X}$,

$$\begin{aligned} \mathcal{E}_{\ell_{\text{def}}}(g, r) - \mathcal{E}_{\ell_{\text{def}}}^B(\mathcal{G}, \mathcal{R}) + \mathcal{U}_{\ell_{\text{def}}}(\mathcal{G}, \mathcal{R}) &\leq \\ \bar{\Gamma}^\nu \left(\mathcal{E}_{\Phi_{\text{def}}^\nu}(r) - \mathcal{E}_{\Phi_{\text{def}}^\nu}^*(\mathcal{R}) + \mathcal{U}_{\Phi_{\text{def}}^\nu}(\mathcal{R}) \right) & \\ + \mathcal{E}_{c_0}(g) - \mathcal{E}_{c_0}^B(\mathcal{G}) + \mathcal{U}_{c_0}(\mathcal{G}), & \end{aligned}$$

where $\bar{\Gamma}^\nu(u) = \|\bar{\tau}\|_1 \Gamma^\nu\left(\frac{u}{\|\bar{\tau}\|_1}\right)$, with $\Gamma^\nu(u) = \mathcal{T}^{-1, \nu}(u)$, and for the log-softmax surrogate, $\mathcal{T}^{\nu=1}(u) = \frac{1+u}{2} \log(1+u) + \frac{1-u}{2} \log(1-u)$.

Proof Let denote a cost for $j \in \mathcal{A} = \{0, \dots, J\}$:

$$\bar{c}_j^* = \begin{cases} \inf_{g \in \mathcal{G}} \mathbb{E}_{y, t|x} [c_0(g(x), z)] & \text{if } j = 0 \\ \mathbb{E}_{y, t|x} [c_j(m(x), z)] & \text{otherwise} \end{cases}$$

Using the change of variables and the Bayes-conditional risk introduced in the proof of Lemma 2 in Appendix B, we have:

$$\begin{aligned} \mathcal{C}_{\ell_{\text{def}}}^B(\mathcal{G}, \mathcal{R}, x) &= \min_{j \in \mathcal{A}} \bar{c}_j^* \\ \mathcal{C}_{\ell_{\text{def}}}(g, r, x) &= \sum_{j=0}^J \mathbb{E}_{y, t|x} [c_j(g(x), m_j(x), z)] \mathbf{1}_{r(x)=j} \end{aligned} \quad (17)$$

We follow suit for our surrogate Φ_{def} and derive its conditional risk and optimal conditional risk.

$$\begin{aligned} \mathcal{C}_{\Phi_{\text{def}}} &= \mathbb{E}_{y, t|x} \left[\sum_{j=1}^J c_j(m(x), z) \Phi_{01}^\nu(r, x, 0) + \sum_{j=1}^J \left(c_0(g(x), z) + \sum_{i=1}^J c_i(m_i(x), z) \mathbf{1}_{j \neq i} \right) \Phi_{01}^\nu(r, x, j) \right] \\ \mathcal{C}_{\Phi_{\text{def}}}^* &= \inf_{r \in \mathcal{R}} \mathbb{E}_{y, t|x} \left[\sum_{j=1}^J c_j(g(x), m(x), z) \Phi_{01}^\nu(r, x, 0) + \sum_{j=1}^J [c_0(g(x), z) + \sum_{i=1}^J c_i(m_i(x), z) \mathbf{1}_{j \neq i}] \Phi_{01}^\nu(r, x, j) \right] \end{aligned}$$

Let us define the function $v(m(x), z) = \min_{j \in [J]} \bar{c}_j(m_j(x), z)$, where $m_j(x)$ denotes the model's output and \bar{c}_j represents the corresponding cost function. Using this definition, the calibration gap is formulated as $\Delta \mathcal{C}_{\ell_{\text{def}}} := \mathcal{C}_{\ell_{\text{def}}} - \mathcal{C}_{\ell_{\text{def}}}^B$, where $\mathcal{C}_{\ell_{\text{def}}}$ represents the original calibration term and $\mathcal{C}_{\ell_{\text{def}}}^B$ denotes the baseline calibration term. By construction, the calibration gap satisfies $\Delta \mathcal{C}_{\ell_{\text{def}}} \geq 0$, leveraging the risks derived in the preceding analysis.

$$\begin{aligned} \Delta \mathcal{C}_{\ell_{\text{def}}} &= \mathbb{E}_{y, t|x} \left[\rho(g(x), z) \mathbf{1}_{r(x)=0} + \sum_{j=1}^J \left(\rho(m(x), z) + \beta_j \right) \mathbf{1}_{r(x)=j} \right] \\ &\quad - v(m(x), z) + \left(v(m(x), z) - \min_{j \in \mathcal{A}} \bar{c}_j^*(g(x), m(x), z) \right) \end{aligned}$$

Let us consider $\Delta \mathcal{C}_{\ell_{\text{def}}} = A_1 + A_2$, such that:

$$\begin{aligned} A_1 &= \mathbb{E}_{y, t|x} \left[\mathbf{1}_{r(x)=0} \rho(g(x), z) + \sum_{j=1}^J \mathbf{1}_{r(x)=j} \left(\rho(m_j(x), z) + \beta_j \right) \right] - v(m(x), z) \\ A_2 &= \left(v(m(x), z) - \min_{j \in \mathcal{A}} \bar{c}_j^*(g(x), m(x), z) \right) \end{aligned} \quad (18)$$

By considering the properties of min, we also get the following inequality:

$$v(m(x), z) - \min_{j \in \mathcal{A}} \bar{c}_j^*(g(x), m(x), z) \leq \mathbb{E}_{y,t|x}[c_0(g(x), z)] - \inf_{g \in \mathcal{G}} \mathbb{E}_{y,t|x}[c_0(g(x), z)] \quad (19)$$

implying,

$$\Delta \mathcal{C}_{\ell_{\text{def}}} \leq A_1 + \bar{c}_0(g(x), z) - \bar{c}_0^*(g(x), z) \quad (20)$$

We now select a distribution for our rejector. We first define $\forall j \in \mathcal{A}$,

$$p_0 = \frac{\sum_{j=1}^J \bar{c}_j(m_j(x), z)}{J \sum_{j=0}^J \bar{c}_j(g(x), m_j(x), z)}$$

and

$$p_{j \in [J]} = \frac{\bar{c}_0(g(x), z) + \sum_{j \neq j'} \bar{c}_j(m_j(x), z)}{J \sum_{j=0}^J \bar{c}_j(g(x), m_j(x), z)}$$

which can also be written as:

$$p_j = \frac{\bar{\tau}_j}{\|\bar{\tau}\|_1} \quad (21)$$

Injecting the new distribution, we obtain the following:

$$\Delta \mathcal{C}_{\Phi_{\text{def}}} = \|\bar{\tau}\|_1 \left(\sum_{j=0}^J p_j \Phi_{01}'(r, x, j) - \inf_{r \in \mathcal{R}} \sum_{j=0}^J p_j \Phi_{01}'(r, x, j) \right) \quad (22)$$

Now consider the first and last term of $\Delta \mathcal{C}_{\ell_{\text{def}}}$. Following the intermediate step for Lemma 3, we have:

$$\begin{aligned} A_1 &= \mathbb{E}_{y,t|x}[c_0(g(x), z)]1_{r(x)=0} + \sum_{j=1}^J \mathbb{E}_{y,t|x}[c_j(m_j(x), z)]1_{r(x)=j} - v(m(x), z) \\ &= \mathbb{E}_{y,t|x}[c_0(g(x), z)]1_{r(x)=0} + \sum_{j=1}^J \mathbb{E}_{y,t|x}[c_j(m_j(x), z)]1_{r(x)=j} \\ &\quad - \inf_{r \in \mathcal{R}} \left[\mathbb{E}_{y,t|x}[c_0(g(x), z)]1_{r(x)=0} + \sum_{j=1}^J \mathbb{E}_{y,t|x}[c_j(m_j(x), z)]1_{r(x)=j} \right] \\ &= \sum_{j=1}^J \bar{c}_j(z, m_j)1_{r(x) \neq 0} + \sum_{j=1}^J \left(\bar{c}_0(g(x), z) + \sum_{j \neq j'} \bar{c}_j(m_{j'}(x), z) \right) 1_{r(x) \neq j} \\ &\quad - \inf_{r \in \mathcal{R}} \left[\sum_{j=1}^J \bar{c}_j(m_{j'}(x), z)1_{r(x) \neq 0} + \sum_{j=1}^J \left(\bar{c}_0(g(x), z) + \sum_{j \neq j'} \bar{c}_j(m_{j'}(x), z) \right) 1_{r(x) \neq j} \right] \end{aligned}$$

Then, applying a change of variables to introduce $\|\bar{\tau}\|_1$, we get:

$$\begin{aligned} &\|\bar{\tau}\|_1 p_0 1_{r(x) \neq 0} + \|\bar{\tau}\|_1 \sum_{j=1}^J p_j 1_{r(x) \neq j} - \inf_{r \in \mathcal{R}} \left[\|\bar{\tau}\|_1 p_0 1_{r(x) \neq 0} + \|\bar{\tau}\|_1 \sum_{j=1}^J p_j 1_{r(x) \neq j} \right] \\ &= \|\bar{\tau}\|_1 \sum_{j=0}^J p_j 1_{r(x) \neq j} - \inf_{r \in \mathcal{R}} \|\bar{\tau}\|_1 \sum_{j=0}^J p_j 1_{r(x) \neq j} \end{aligned}$$

We now apply Lemma 9 to introduce Γ ,

$$\begin{aligned} \sum_{j=0}^J p_j 1_{r(x) \neq j} - \inf_{r \in \mathcal{R}} \sum_{j=0}^J p_j 1_{r(x) \neq j} &\leq \Gamma \left(\sum_{j=0}^J p_j \Phi_{01}^\nu(r, x, j) - \inf_{r \in \mathcal{R}} \sum_{j=0}^J p_j \Phi_{01}^\nu(r, x, j) \right) \\ \frac{1}{\|\bar{\tau}\|_1} \left[\sum_{j=0}^J \bar{\tau}_j 1_{r(x) \neq j} - \inf_{r \in \mathcal{R}} \sum_{j=0}^J \bar{\tau}_j 1_{r(x) \neq j} \right] &\leq \Gamma \left(\frac{1}{\|\bar{\tau}\|_1} \left[\sum_{j=0}^J \bar{\tau}_j \Phi_{01}^\nu(r, x, j) - \inf_{r \in \mathcal{R}} \sum_{j=0}^J \bar{\tau}_j \Phi_{01}^\nu(r, x, j) \right] \right) \\ \Delta \mathcal{C}_{\ell_{\text{def}}} &\leq \|\bar{\tau}\|_1 \Gamma \left(\frac{\Delta \mathcal{C}_{\Phi_{\text{def}}}}{\|\bar{\tau}\|_1} \right) \end{aligned} \tag{23}$$

We reintroduce the coefficient A_2 such that:

$$\begin{aligned} \Delta \mathcal{C}_{\ell_{\text{def}}} &\leq \|\bar{\tau}\|_1 \Gamma \left(\frac{\Delta \mathcal{C}_{\Phi_{\text{def}}}}{\|\bar{\tau}\|_1} \right) + A_2 \\ \Delta \mathcal{C}_{\ell_{\text{def}}} &\leq \|\bar{\tau}\|_1 \Gamma \left(\frac{\Delta \mathcal{C}_{\Phi_{\text{def}}}}{\|\bar{\tau}\|_1} \right) + \mathbb{E}_{y,t|x} [c_0(g(x), z)] - \inf_{g \in \mathcal{G}} \mathbb{E}_{y,t|x} [c_0(g(x), z)] \quad (\text{upper bounding with Eq 19}) \end{aligned}$$

Mao et al. (2023b) introduced a tight bound for the comp-sum surrogates family. It follows for $\nu \geq 0$ the inverse transformation $\Gamma^\nu(u) = \mathcal{T}^{-1,\nu}(u)$:

$$\mathcal{T}^\nu(v) = \begin{cases} \frac{2^{1-\nu}}{1-\nu} \left[1 - \left(\frac{(1+v)^{\frac{2-\nu}{2}} + (1-v)^{\frac{2-\nu}{2}}}{2} \right)^{2-\nu} \right] & \nu \in [0, 1) \\ \frac{1+v}{2} \log[1+v] + \frac{1-v}{2} \log[1-v] & \nu = 1 \\ \frac{1}{(\nu-1)n^{\nu-1}} \left[\left(\frac{(1+v)^{\frac{2-\nu}{2}} + (1-v)^{\frac{2-\nu}{2}}}{2} \right)^{2-\nu} - 1 \right] & \nu \in (1, 2) \\ \frac{1}{(\nu-1)n^{\nu-1}} v & \nu \in [2, +\infty). \end{cases}$$

We note $\bar{\Gamma}^\nu(u) = \|\bar{\tau}\|_1 \Gamma^\nu\left(\frac{u}{\|\bar{\tau}\|_1}\right)$. By applying Jensen's Inequality and taking expectation on both sides, we get

$$\begin{aligned} \mathcal{E}_{\ell_{\text{def}}}(g, r) - \mathcal{E}_{\ell_{\text{def}}}^B(\mathcal{G}, \mathcal{R}) + \mathcal{U}_{\ell_{\text{def}}}(\mathcal{G}, \mathcal{R}) \\ \leq \bar{\Gamma}^\nu(\mathcal{E}_{\Phi_{\text{def}}}(r) - \mathcal{E}_{\Phi_{\text{def}}}^*(\mathcal{R}) + \mathcal{U}_{\Phi_{\text{def}}}(\mathcal{R})) + \mathcal{E}_{c_0}(g) - \mathcal{E}_{c_0}^B(\mathcal{G}) + \mathcal{U}_{c_0}(\mathcal{G}) \end{aligned}$$

■

Appendix D. Proof Theorem 6

Theorem 6 (Characterization Minimability Gaps). *Assume \mathcal{R} symmetric and complete. Then, for the cross-entropy multiclass surrogates Φ_{01}^ν and any distribution \mathcal{D} , it follows for*

$\nu \geq 0$:

$$\mathcal{C}_{\Phi_{\text{def}}}^{\nu,*} = \begin{cases} \|\bar{\tau}\|_1 H\left(\frac{\bar{\tau}}{\|\bar{\tau}\|_1}\right) & \nu = 1 \\ \|\bar{\tau}\|_1 - \|\bar{\tau}\|_\infty & \nu = 2 \\ \frac{1}{\nu-1} \left[\|\bar{\tau}\|_1 - \|\bar{\tau}\|_{\frac{1}{2-\nu}} \right] & \nu \in (1, 2) \\ \frac{1}{1-\nu} \left[\left(\sum_{k=0}^J \bar{\tau}_k^{\frac{1}{2-\nu}} \right)^{2-\nu} - \|\bar{\tau}\|_1 \right] & \text{otherwise,} \end{cases}$$

then the minimizability gap is,

$$\mathcal{U}_{\Phi_{\text{def}}}^{\nu}(\mathcal{R}) = \mathcal{E}_{\Phi_{\text{def}}}^*(\mathcal{R}) - \mathbb{E}_x[\inf_{r \in \mathcal{R}} \mathcal{C}_{\Phi_{\text{def}}}^{\nu}(r, x)]$$

with $\bar{\tau} = \{\mathbb{E}_{y,t|x}[\bar{\tau}_0], \dots, \mathbb{E}_{y,t|x}[\bar{\tau}_J]\}$, the aggregated costs $\tau_j = \sum_{k=0}^J c_k 1_{k \neq j}$, and the Shannon Entropy H .

Proof

We define the softmax distribution as $s_j = \frac{e^{r(x,j)}}{\sum_{j' \in \mathcal{A}} e^{r(x,j')}}$, where $s_j \in [0, 1]$. Let $\bar{\tau}_j = \bar{\tau}_j(g(x), m(x), z)$ with $\tau_j \in \mathbb{R}^+$, and denote the expected value as $\bar{\tau} = \mathbb{E}_{y,t|x}[\tau]$. We now derive the conditional risk for a given $\nu \geq 0$:

$$\begin{aligned} \mathcal{C}_{\Phi_{\text{def}}}^{\nu}(r, x) &= \sum_{j=0}^J \mathbb{E}_{y,t|x}[\tau_j] \Phi_{01}^{\nu}(r, x, j) \\ &= \begin{cases} \frac{1}{1-\nu} \sum_{j=0}^J \bar{\tau}_j \left[\left(\sum_{j' \in \mathcal{A}} e^{r(x,j') - r(x,j)} \right)^{1-\nu} - 1 \right] & \nu \neq 1 \\ \sum_{j=0}^J \bar{\tau}_j \log \left(\sum_{j' \in \mathcal{A}} e^{r(x,j') - r(x,j)} \right) & \nu = 1 \end{cases} \quad (24) \\ &= \begin{cases} \frac{1}{1-\nu} \sum_{j=0}^J \bar{\tau}_j \left[s_j^{\nu-1} - 1 \right] & \nu \neq 1 \\ - \sum_{j=0}^J \bar{\tau}_j \log(s_j) & \nu = 1 \end{cases} \end{aligned}$$

For $\nu = 1$: we can write the following conditional risk:

$$\mathcal{C}_{\Phi_{\text{def}}}^{\nu=1}(r, x) = - \sum_{j=0}^J \bar{\tau}_j \left[r(x, j) - \log \sum_{j' \in \mathcal{A}} e^{r(x,j')} \right] \quad (25)$$

Then,

$$\frac{\partial \mathcal{C}_{\Phi_{\text{def}}}^{\nu=1}}{\partial r(x, i)}(r, x) = -\bar{\tau}_i + \left(\sum_{j=0}^J \bar{\tau}_j \right) s_i^* \quad (26)$$

At the optimum, we have:

$$s^*(x, i) = \frac{\bar{\tau}_i}{\sum_{j=0}^J \bar{\tau}_j} \quad (27)$$

Then, it follows:

$$\mathcal{C}_{\Phi_{\text{def}}}^{*,\nu=1}(\mathcal{R}, x) = - \sum_{j=0}^J \bar{\tau}_j \log \left(\frac{\bar{\tau}_j}{\sum_{j'=0}^J \bar{\tau}_{j'}} \right) \quad (28)$$

As the softmax parametrization is a distribution $s^* \in \Delta^{|\mathcal{A}|}$, we can write this conditional in terms of entropy with $\bar{\tau} = \{\bar{\tau}_j\}_{j \in \mathcal{A}}$:

$$\begin{aligned} \mathcal{C}_{\Phi_{\text{def}}}^{*, \nu=1}(\mathcal{R}, x) &= - \left(\sum_{k=0}^J \bar{\tau}_k \right) \sum_{j=0}^J s_j^* \log(s_j^*) \\ &= \left(\sum_{k=0}^J \bar{\tau}_k \right) H \left(\frac{\bar{\tau}}{\sum_{j'=0}^J \bar{\tau}_{j'}} \right) \\ &= \|\bar{\tau}\|_1 H \left(\frac{\bar{\tau}}{\|\bar{\tau}\|_1} \right) \quad (\text{as } \tau_j \in \mathbb{R}^+) \end{aligned} \quad (29)$$

For $\nu \neq 1, 2$: The softmax parametrization can be written as a constraint $\sum_{j=0}^J s_j = 1$ and $s_j \geq 0$. Consider the objective

$$\Phi(\mathbf{s}) = \frac{1}{1-\nu} \sum_{j=0}^J \bar{\tau}_j \left[s_j^{\nu-1} - 1 \right]. \quad (30)$$

We aim to find $\mathbf{s}^* = (s_0^*, \dots, s_J^*)$ that minimizes (30) subject to $\sum_{j=0}^J s_j = 1$. Introduce a Lagrange multiplier λ for the normalization $\sum_{j=0}^J s_j = 1$. The Lagrangian is:

$$\mathcal{L}(\mathbf{s}, \lambda) = \frac{1}{1-\nu} \sum_{j=0}^J \bar{\tau}_j [s_j^{\nu-1} - 1] + \lambda \left(1 - \sum_{j=0}^J s_j \right). \quad (31)$$

We take partial derivatives with respect to s_i :

$$\frac{\partial \mathcal{L}}{\partial s_i} = \frac{1}{1-\nu} \bar{\tau}_i (\nu-1) s_i^{\nu-2} - \lambda = 0. \quad (32)$$

Since $\frac{\nu-1}{1-\nu} = -1$, we get

$$\bar{\tau}_i s_i^{\nu-2} = -\lambda > 0 \implies s_i^{\nu-2} = \frac{\alpha}{\bar{\tau}_i} \text{ for some } \alpha > 0. \quad (33)$$

Hence

$$s_i = \left(\frac{\alpha}{\bar{\tau}_i} \right)^{\frac{1}{\nu-2}}. \quad (34)$$

Summing s_i over $\{i = 0, \dots, J\}$ and setting the total to 1 yields:

$$\sum_{i=0}^J \left(\frac{\alpha}{\bar{\tau}_i} \right)^{\frac{1}{\nu-2}} = 1. \quad (35)$$

Let

$$\alpha^{\frac{1}{\nu-2}} = \frac{1}{\sum_{k=0}^J \left(\frac{1}{\bar{\tau}_k} \right)^{\frac{1}{\nu-2}}} \implies \alpha = \left[\sum_{k=0}^J \left(\frac{1}{\bar{\tau}_k} \right)^{\frac{1}{\nu-2}} \right]^{\nu-2}. \quad (36)$$

Therefore, for each i ,

$$s_i^* = \left(\frac{\alpha}{\bar{\tau}_i}\right)^{\frac{1}{\nu-2}} = \frac{\bar{\tau}_i^{\frac{1}{2-\nu}}}{\sum_{k=0}^J \bar{\tau}_k^{\frac{1}{2-\nu}}}. \quad (37)$$

This $\{s_i^*\}$ is a valid probability distribution. Let

$$A = \sum_{k=0}^J \bar{\tau}_k^{\frac{1}{2-\nu}}. \quad (38)$$

Then the optimum distribution is

$$s_i^* = \frac{\bar{\tau}_i^{\frac{1}{2-\nu}}}{A}. \quad (39)$$

Recall

$$\Phi(\mathbf{s}) = \frac{1}{1-\nu} \sum_{j=0}^J \bar{\tau}_j \left[s_j^{\nu-1} - 1 \right]. \quad (40)$$

At s_j^* , we have

$$(s_j^*)^{\nu-1} = \left(\frac{\bar{\tau}_j^{\frac{1}{2-\nu}}}{A}\right)^{\nu-1} = \frac{\bar{\tau}_j^{\frac{\nu-1}{2-\nu}}}{A^{\nu-1}}. \quad (41)$$

Hence

$$\sum_{j=0}^J \bar{\tau}_j (s_j^*)^{\nu-1} = \frac{1}{A^{\nu-1}} \sum_{j=0}^J \bar{\tau}_j^{1+\frac{\nu-1}{2-\nu}} = \frac{1}{A^{\nu-1}} \sum_{j=0}^J \bar{\tau}_j^{\frac{1}{2-\nu}} = \frac{A}{A^{\nu-1}} = A^{2-\nu}. \quad (42)$$

Substituting back,

$$\mathcal{C}_{\Phi_{\text{def}}}^{*,\nu \neq 1,2}(\mathcal{R}, x) = \frac{1}{1-\nu} \left[\left(\sum_{k=0}^J \bar{\tau}_k^{\frac{1}{2-\nu}} \right)^{2-\nu} - \sum_{j=0}^J \bar{\tau}_j \right] \quad (43)$$

We can express this conditional risk with a valid $L^{(\frac{1}{2-\nu})}$ norm as long as $\nu \in (1, 2)$.

$$\mathcal{C}_{\Phi_{\text{def}}}^{*,\nu \neq 1,2}(\mathcal{R}, x) = \frac{1}{\nu-1} \left[\|\bar{\tau}\|_1 - \|\bar{\tau}\|_{\frac{1}{2-\nu}} \right] \quad (44)$$

For $\nu = 2$: Since $\sum_{j=0}^J \bar{\tau}_j = S$, we have

$$\mathcal{C}_{\Phi_{\text{def}}}^{\nu=2}(r, x) = \sum_{j=0}^J \bar{\tau}_j [1 - s_j(r)] = \sum_{j=0}^J \bar{\tau}_j - \sum_{j=0}^J \bar{\tau}_j s_j(r). \quad (45)$$

Hence

$$\inf_{r \in \mathcal{R}} \mathcal{C}_{\Phi_{\text{def}}}^{\nu=2}(r, x) = S - \sup_{r \in \mathcal{R}} \sum_{j=0}^J \bar{\tau}_j s_j(r). \quad (46)$$

Therefore, minimizing $\mathcal{C}_{\Phi_{\text{def}}}^{\nu=2}(r, x)$ is equivalent to maximizing

$$F(r) = \sum_{j=0}^J \bar{\tau}_j s_j(r). \quad (47)$$

Its partial derivative w.r.t. r_i is the standard softmax derivative:

$$\frac{\partial s_j}{\partial r_i} = s_j (\delta_{ij} - s_i) = \begin{cases} s_i (1 - s_i), & \text{if } i = j, \\ -s_j s_i, & \text{otherwise.} \end{cases} \quad (48)$$

Hence, for each i ,

$$\frac{\partial F}{\partial r_i} = \sum_{j=0}^J \bar{\tau}_j \frac{\partial s_j}{\partial r_i} = \bar{\tau}_i s_i (1 - s_i) + \sum_{\substack{j=0 \\ j \neq i}}^J \bar{\tau}_j (-s_j s_i). \quad (49)$$

Factor out s_i :

$$\frac{\partial F}{\partial r_i} = s_i \left[\bar{\tau}_i (1 - s_i) - \sum_{j \neq i} \bar{\tau}_j s_j \right] = s_i \left[\bar{\tau}_i - \left(\sum_{j=0}^J \bar{\tau}_j s_j \right) \right], \quad (50)$$

because $\sum_{j \neq i} \bar{\tau}_j s_j = \sum_{j=0}^J \bar{\tau}_j s_j - \bar{\tau}_i s_i$. Define $F(r) = \sum_{j=0}^J \bar{\tau}_j s_j(r)$. Then:

$$\frac{\partial F}{\partial r_i} = s_i [\bar{\tau}_i - F(r)]. \quad (51)$$

Setting $\frac{\partial F}{\partial r_i} = 0$ for each i implies

$$s_i [\bar{\tau}_i - F(r)] = 0, \quad \forall i. \quad (52)$$

Thus, for each index i :

$$s_i = 0 \quad \text{or} \quad \bar{\tau}_i = F(r). \quad (53)$$

To maximize $F(r)$, notice that:

- If $\bar{\tau}_{i^*}$ is strictly the largest among all $\bar{\tau}_i$, then the maximum is approached by making $s_{i^*} \approx 1$, so $F(r) \approx \bar{\tau}_{i^*}$. In the softmax parameterization, this occurs in the limit $r_{i^*} \rightarrow +\infty$ and $r_k \rightarrow -\infty$ for $k \neq i^*$.
- If there is a tie for the largest $\bar{\tau}_i$, we can put mass on those coordinates that share the maximum value. In any case, the supremum is $\max_i \bar{\tau}_i$.

Hence

$$\sup_{r \in \mathcal{R}} F(r) = \max_{0 \leq i \leq J} \bar{\tau}_i. \quad (54)$$

Because $\mathcal{C}_{\Phi_{\text{def}}}^{\nu=2}(r, x) = S - F(r)$,

$$\inf_{r \in \mathcal{R}} \mathcal{C}_{\Phi_{\text{def}}}^{\nu=2}(r, x) = S - \sup_{r \in \mathcal{R}} F(r) = \sum_{j=0}^J \bar{\tau}_j - \max_{i \in \mathcal{A}} \bar{\tau}_i = \|\bar{\boldsymbol{\tau}}\|_1 - \|\bar{\boldsymbol{\tau}}\|_\infty \quad (55)$$

Hence the global minimum of $\mathcal{C}_{\Phi_{\text{def}}}^{\nu=2}$ is $\|\bar{\tau}\|_1 - \|\bar{\tau}\|_\infty$. In the ‘‘softmax’’ parameterization, this is only approached in the limit as one coordinate r_{i^*} goes to $+\infty$ and all others go to $-\infty$. No finite r yields an exactly one-hot $s_i(r) = 1$, but the limit is enough to achieve the infimum arbitrarily closely.

It follows for $\bar{\tau} = \{\bar{\tau}_j\}_{j \in \mathcal{A}}$ and $\nu \geq 0$:

$$\inf_{r \in \mathcal{R}} \mathcal{C}_{\Phi_{\text{def}}}^\nu(r, x) = \begin{cases} \|\bar{\tau}\|_1 H\left(\frac{\bar{\tau}}{\|\bar{\tau}\|_1}\right) & \nu = 1 \\ \|\bar{\tau}\|_1 - \|\bar{\tau}\|_\infty & \nu = 2 \\ \frac{1}{\nu-1} \left[\|\bar{\tau}\|_1 - \|\bar{\tau}\|_{\frac{1}{2-\nu}} \right] & \nu \in (1, 2) \\ \frac{1}{1-\nu} \left[\left(\sum_{k=0}^J \bar{\tau}_k \frac{1}{2-\nu} \right)^{2-\nu} - \|\bar{\tau}\|_1 \right] & \text{otherwise} \end{cases} \quad (56)$$

Building on this, we can infer the minimizability gap:

$$\mathcal{U}_{\Phi_{\text{def}}}(\mathcal{R}) = \mathcal{E}_{\Phi_{\text{def}}}^*(\mathcal{R}) - \mathbb{E}_x \left[\inf_{r \in \mathcal{R}} \mathcal{C}_{\Phi_{\text{def}}}^\nu(r, x) \right] \quad (57)$$

■

Appendix E. Proof Lemma 7

Lemma 7. *Let \mathcal{L}_1 be a family of functions mapping \mathcal{X} to $[0, 1]$, and let \mathcal{L}_2 be a family of functions mapping \mathcal{X} to $\{0, 1\}$. Define $\mathcal{L} = \{l_1 l_2 : l_1 \in \mathcal{L}_1, l_2 \in \mathcal{L}_2\}$. Then, the empirical Rademacher complexity of \mathcal{L} for any sample S of size K is bounded by:*

$$\hat{\mathfrak{R}}_S(\mathcal{L}) \leq \hat{\mathfrak{R}}_S(\mathcal{L}_1) + \hat{\mathfrak{R}}_S(\mathcal{L}_2). \quad (7)$$

Proof We define the function ψ as follows:

$$\psi : \begin{array}{ll} \mathcal{L}_1 + \mathcal{L}_2 & \longrightarrow \mathcal{L}_1 \mathcal{L}_2 \\ l_1 + l_2 & \longmapsto (l_1 + l_2 - 1)_+ \end{array} \quad (58)$$

Here, $l_1 \in \mathcal{L}_1$ and $l_2 \in \mathcal{L}_2$. The function ψ is 1-Lipschitz as we have $t \mapsto (t - 1)_+$ for $t = l_1 + l_2$. Furthermore, given that ψ is surjective and 1-Lipschitz, by Talagrand’s lemma (Mohri et al., 2012), we have:

$$\hat{\mathfrak{R}}_S(\psi(\mathcal{L}_1 + \mathcal{L}_2)) \leq \hat{\mathfrak{R}}_S(\mathcal{L}_1 + \mathcal{L}_2) \leq \hat{\mathfrak{R}}_S(\mathcal{L}_1) + \hat{\mathfrak{R}}_S(\mathcal{L}_2) \quad (59)$$

This inequality shows that the Rademacher complexity of the sum of the losses is bounded by the sum of their individual complexities. ■

Appendix F. Proof Theorem 8

Theorem 8 (Learning bounds of the deferral loss). *For any expert M_j , any distribution \mathcal{D} over \mathcal{Z} , we have with probability $1 - \delta$ for $\delta \in [0, 1/2]$, that the following bound holds at the optimum:*

$$\mathcal{E}_{\ell_{\text{def}}}(h, f, r) \leq \hat{\mathcal{E}}_{\ell_{\text{def}}}(h, f, r) + 2\mathfrak{R}_K(\mathcal{L}_{\text{def}}) + \sqrt{\frac{\log 1/\delta}{2K}},$$

with

$$\begin{aligned} \mathfrak{R}_K(\mathcal{L}_{def}) &\leq \frac{1}{2}\mathfrak{R}_K(\mathcal{H}) + \mathfrak{R}_K(\mathcal{F}) + \sum_{j=1}^J \Omega(m_j^h, y) \\ &\quad + \left(\sum_{j=1}^J \max_t \ell_{reg}(m_j^f, t) + 2 \right) \mathfrak{R}_K(\mathcal{R}), \end{aligned}$$

with $\Omega(m_j^h, y) = \frac{1}{2}\mathcal{D}(m_j^h \neq y) \exp\left(-\frac{K}{8}\mathcal{D}(m_j^h \neq y)\right) + \mathcal{R}_{K\mathcal{D}(m_j^h \neq y)/2}(\mathcal{R})$.

Proof

We are interested in finding the generalization of $u = (g, r) \in \mathcal{L}$:

$$\begin{aligned} \mathfrak{R}_S(\mathcal{L}) &= \frac{1}{K} \mathbb{E}_\sigma \left[\sup_{g \in \mathcal{L}} \sum_{k=1}^K \sigma_k \ell_{def}(g, r, x_k, y_k, b_k, m_k) \right] \\ &= \frac{1}{K} \mathbb{E}_\sigma \left[\sup_{g \in \mathcal{L}} \sum_{k=1}^K \sigma_k \left(\sum_{j=0}^J c_j 1_{r(x_k)=j} \right) \right] \\ &\leq \frac{1}{K} \mathbb{E}_\sigma \left[\sup_{g \in \mathcal{L}} \sum_{k=1}^K \sigma_k c_0 1_{r(x_k)=0} \right] + \frac{1}{K} \sum_{j=1}^J \mathbb{E}_\sigma \left[\sup_{r \in \mathcal{R}} \sum_{k=1}^K \sigma_k c_j 1_{r(x_k)=j} \right] \quad (\text{By the subadditivity of sup}) \end{aligned}$$

Let's consider $j = 0$:

$$\begin{aligned} \frac{1}{K} \mathbb{E}_\sigma \left[\sup_{g \in \mathcal{L}} \sum_{k=1}^K \sigma_k c_0 1_{r(x_k)=0} \right] &= \frac{1}{K} \mathbb{E}_\sigma \left[\sup_{g \in \mathcal{L}} \sum_{k=1}^K \sigma_k [1_{h(x_k) \neq y} + \ell_{reg}(f(x_k), b_k)] 1_{r(x_k)=0} \right] \\ &\leq \frac{1}{K} \mathbb{E}_\sigma \left[\sup_{g \in \mathcal{L}} \sum_{k=1}^K \sigma_k 1_{h(x_k) \neq y} 1_{r(x_k)=0} \right] + \frac{1}{K} \mathbb{E}_\sigma \left[\sup_{g \in \mathcal{L}} \sum_{k=1}^K \sigma_k \ell_{reg}(f(x_k), b_k) 1_{r(x_k)=0} \right] \\ &\leq \left[\frac{1}{2} \mathfrak{R}_K(\mathcal{H}) + \mathfrak{R}_K(\mathcal{R}) \right] + \left[\mathfrak{R}_K(\mathcal{F}) + \mathfrak{R}_K(\mathcal{R}) \right] \quad (\text{using Lemma 7}) \\ &= \frac{1}{2} \mathfrak{R}_K(\mathcal{H}) + \mathfrak{R}_K(\mathcal{F}) + 2\mathfrak{R}_K(\mathcal{R}) \end{aligned} \tag{60}$$

Let's consider $j > 0$:

$$\begin{aligned} \frac{1}{K} \sum_{j=1}^J \mathbb{E}_\sigma \left[\sup_{r \in \mathcal{R}} \sum_{k=1}^K \sigma_k c_j 1_{r(x_k)=j} \right] &\leq \frac{1}{K} \sum_{j=1}^J \mathbb{E}_\sigma \left[\sup_{r \in \mathcal{R}} \sum_{k=1}^K \sigma_k 1_{m_{k,j}^h \neq y} 1_{r(x_k)=j} \right] \\ &\quad + \frac{1}{K} \sum_{j=1}^J \mathbb{E}_\sigma \left[\sup_{r \in \mathcal{R}} \sum_{k=1}^K \sigma_k \ell_{reg}(m_{k,j}^f, b_k) 1_{r(x_k)=j} \right] \end{aligned} \tag{61}$$

Using learning-bounds for single expert in classification (Mozannar and Sontag, 2020), we have:

$$\frac{1}{K} \mathbb{E}_\sigma \left[\sup_{r \in \mathcal{R}} \sum_{k=1}^K \sigma_k 1_{m_k^h \neq y} 1_{r(x_k)=1} \right] \leq \frac{\mathcal{D}(m^h \neq y)}{2} \exp\left(-\frac{K\mathcal{D}(m^h \neq y)}{8}\right) + \mathcal{R}_{K\mathcal{D}(m^h \neq y)/2}(\mathcal{R}) \tag{62}$$

Applying it to our case:

$$\frac{1}{K} \sum_{j=1}^J \mathbb{E}_\sigma \left[\sup_{r \in \mathcal{R}} \sum_{k=1}^K \sigma_k \mathbf{1}_{m_{k,j}^h \neq y} \mathbf{1}_{r(x_k)=j} \right] \leq \sum_{j=1}^J \left(\frac{\mathcal{D}(m_j^h \neq y)}{2} \exp \left(-\frac{K\mathcal{D}(m_j^h \neq y)}{8} \right) + \mathcal{R}_{K\mathcal{D}(m_j^h \neq y)/2}(\mathcal{R}) \right) \quad (63)$$

For the last term,

$$\frac{1}{K} \sum_{j=1}^J \mathbb{E}_\sigma \left[\sup_{r \in \mathcal{R}} \sum_{k=1}^K \sigma_k \ell_{\text{reg}}(m_{k,j}^f, b_k) \mathbf{1}_{r(x_k)=j} \right] \leq \sum_{j=1}^J \left(\max \ell_{\text{reg}}(m_j^f, t) \mathfrak{R}_K(\mathcal{R}) \right) \quad (64)$$

Then, it leads to:

$$\mathfrak{R}_K(\mathcal{L}_{\text{def}}) \leq \frac{1}{2} \mathfrak{R}_K(\mathcal{H}) + \mathfrak{R}_K(\mathcal{F}) + \sum_{j=1}^J \Omega(m_j^h, y) + \left(\sum_{j=1}^J \max \ell_{\text{reg}}(m_j^f, t) + 2 \right) \mathfrak{R}_K(\mathcal{R})$$

with $\Omega(m_j^h, y) = \frac{\mathcal{D}(m_j^h \neq y)}{2} \exp \left(-\frac{K\mathcal{D}(m_j^h \neq y)}{8} \right) + \mathcal{R}_{K\mathcal{D}(m_j^h \neq y)/2}(\mathcal{R})$ ■

Appendix G. Experiments

G.1 PascalVOC Experiment

Since an image may contain multiple objects, our deferral rule is applied at the level of the entire image $x \in \mathcal{X}$, ensuring that the approach remains consistent with real-world scenarios.

	Model	M ₁	M ₂
mAP	39.5	43.3	52.8

Table 2: Agent accuracies on the CIFAR-100 validation set. Since the training and validation sets are pre-determined in this dataset, the agents’ knowledge remains fixed throughout the evaluation.

Cost β_2	mAP (%)	Model Allocation (%)	Expert 1 Allocation (%)	Expert 2 Allocation (%)
0.01	52.8 ± 0.0	0.0 ± 0.0	0.0 ± 0.0	100.0 ± 0.0
0.05	52.5 ± 0.1	7.3 ± 0.8	0.0 ± 0.0	92.7 ± 0.3
0.1	49.1 ± 0.6	48.0 ± 0.7	0.0 ± 0.0	52.0 ± 0.2
0.15	44.2 ± 0.4	68.1 ± 0.3	19.7 ± 0.4	12.2 ± 0.1
0.2	42.0 ± 0.2	77.5 ± 0.2	22.5 ± 0.5	0.0 ± 0.0
0.3	40.1 ± 0.2	98.1 ± 0.0	1.9 ± 0.1	0.0 ± 0.0
0.5	39.5 ± 0.0	100.0 ± 0.0	0.0 ± 0.0	0.0 ± 0.0

Table 3: Detailed results across different cost values β_2 . Errors represent the standard deviation over multiple runs.

G.2 MIMIC-IV Experiments

MIMIC-IV (Johnson et al., 2023) is a large collection of de-identified health-related data covering over forty thousand patients who stayed in critical care units. This dataset includes a wide variety of information, such as demographic details, vital signs, laboratory test results, medications, and procedures. For our analysis, we focus specifically on features related to *procedures*, which correspond to medical procedures performed during hospital visits, and *diagnoses* received by the patients.

Using these features, we address two predictive tasks: (1) a classification task to predict whether a patient will die during their next hospital visit based on clinical information from the current visit, and (2) a regression task to estimate the length of stay for the current hospital visit based on the same clinical information.

A key challenge in this task is the severe class imbalance, particularly in predicting mortality. To mitigate this issue, we sub-sample the negative mortality class, retaining a balanced dataset with $K = 5995$ samples, comprising 48.2% positive mortality cases and 51.8% negative mortality cases. Our model is trained on 80% of this dataset, while the remaining 20% is held out for validation. To ensure consistency in the results, we fixed the training and validation partitions.

	Model	M ₁	M ₂
Accuracy	60.0	39.7	46.2
Smooth L1	1.45	2.31	1.92

Table 4: Performance of the agents on the MIMIC-IV dataset, evaluated in terms of accuracy and Smooth L1 loss. We fixed the training/validation set such that the agents’ knowledge remains fixed throughout the evaluation.

This figure "mimic_4cluster_distribution_training.png" is available in "png" format f

<http://arxiv.org/ps/2410.15729v3>

This figure "mimic_4cluster_distribution_validation.png" is available in "png" format

<http://arxiv.org/ps/2410.15729v3>